

# Uncertainties of drift coefficients and extrapolation errors: Application to clock error prediction

*F. Vernotte<sup>1</sup>, J. Delporte<sup>2</sup>, M. Brunet<sup>2</sup> and T. Tournier<sup>2</sup>*

**Abstract.** In Global Navigation Satellite Systems, the on-board time has to be modeled and predicted in order to broadcast the time parameters to final users. As a consequence, the time prediction performance of the on-board clocks has to be characterized.

In order to estimate the time uncertainty of the on-board oscillator, a linear or parabolic fit is performed over the sequence of observed time difference and extrapolated during the prediction period. In 1998, CNES proposed specifications of orbit determination and time synchronization for GNSS-2. The needs of synchronization were specified as the maximum error of the time difference prediction from the extrapolated fit.

The purpose of this paper is the estimation of this error for different types of noise. This is achieved by the theoretical calculation of the variances of the drifts coefficients, of the residuals and of the extrapolation errors in the case of quadratic and linear drift models affected by different types of red noises.

After the description of the method and its results, examples are given using real data and the predicted extrapolation uncertainties are compared to the real extrapolation errors.

---

<sup>1</sup>F. Vernotte: Laboratoire d'Astrophysique de l'Observatoire de Besançon (LAOB), UPRES-A CNRS 6091, Observatoire de Besançon, 41 bis avenue de l'Observatoire, BP 1615, 25010 Besançon Cedex, FRANCE.

E-mail: francois@obs-besancon.fr

<sup>2</sup>J. Delporte, M. Brunet and T. Tournier: Centre National d'Études Spatiales, 18 avenue Edouard Belin, 31401 Toulouse Cedex 4, FRANCE.

E-mail: jerome.delporte@cnes.fr

## 1 Introduction

In Global Navigation Satellite Systems, the on-board time has to be modeled and predicted in order to broadcast the time parameters to final users. As a consequence, the time prediction performance of the on-board clocks has to be characterized.

In order to estimate the time uncertainty of the on-board oscillator, a linear or parabolic fit is performed over the sequence of observed time difference and extrapolated during the prediction period, i. e. when the satellite is out of visibility. In 1998, CNES proposed specifications of orbit determination and time synchronization for GNSS-2. The needs of synchronization were specified as the maximum error of the time difference prediction from the extrapolated fit.

[Figure 1 about here.]

The question is then: how is this maximum error related to the noise levels of the clock ? Despite several papers deal with this question [1, 2, 3, 4, 5, 6], a new approach was chosen here because we are not only interested in the asymptotic trend of this maximum deviation but also in its evolution close to the interpolated sequence.

In this paper, we will call Time Interval Error (TIE) the differences between the extrapolated parabola and the real time deviation  $x(t)$  (see figure 1, above). By definition, the TIE samples are then the residuals to this parabola (see figure 1, below). However, in the following, we will limit the use of the word “residuals” to the differences between the **interpolated** parabola and the real time deviation  $x(t)$ .

[Figure 2 about here.]

The TIE is due to two effects: the error of determination of the parabolic parameters and the error due the noise of the clock. Obviously, both of these errors may be positive or negative, and the ensemble average of the TIE is equal to zero (see figure 2, above). Moreover, it can be easily shown that the statistics of the TIE

is Gaussian (see figure 2, below). Consequently, we only have to estimate the variance of the TIE in order to completely define its statistical characteristics.

Moreover, the removal of a quadratic fit from the time deviation sequence cancels out the non-stationarity problem of very low frequency noises (see the moment condition in section 2.5 and in [7]), and the variance of the TIE (i.e. the “true variance”) converges for all types of noise without considering an hypothetical low cut-off frequency.

In order to determine an estimation of the TIE, we will already redefine the interpolation method. Then, we will compare the equations giving the theoretical estimates of the variance of the TIE to simulations and to real data.

## 2 Interpolation with the Tchebychev polynomials

### 2.1 Interpolating functions

Let us consider a sequence of  $N$  time deviation data  $x(t)$ , regularly spaced with a sampling period  $\tau_0$ :

$\{x(t_0), x(t_1), \dots, x(t_{N-1})\}$ , and  $t_i = i\tau_0$ .

Rather than carrying out a classical quadratic least squares interpolation:

$$x(t) = C_0 + C_1t + C_2t^2 + e(t) \quad (1)$$

where  $e(t)$  is the noise, i.e. the purely random behavior of  $x(t)$ , we use the first three Tchebychev polynomials

[7, 8] as interpolating functions (see figure 3):

$$\left\{ \begin{array}{l} \Phi_0(t) = \frac{1}{\sqrt{N}} \\ \Phi_1(t) = \sqrt{\frac{3}{(N-1)N(N+1)}} \left[ 2\frac{t}{\tau_0} - (N-1) \right] \\ \Phi_2(t) = \sqrt{\frac{5}{(N-2)(N-1)N(N+1)(N+2)}} \left[ 6\frac{t^2}{\tau_0^2} - 6(N-1)\frac{t}{\tau_0} + (N-2)(N-1) \right]. \end{array} \right. \quad (2)$$

[Figure 3 about here.]

The interpolation we want to perform is then:

$$x(t) = P_0\Phi_0(t) + P_1\Phi_1(t) + P_2\Phi_2(t) + e(t). \quad (3)$$

where all the parameters  $\{P_0, P_1, P_2\}$  have the same dimension as  $x(t)$ , i.e. a time.

Besides their dimensionless nature, the advantage of using these interpolating functions is related to their normality and orthogonality which greatly simplify and improve the estimation of the parameters  $P_0$ ,  $P_1$  and  $P_2$  as well as their statistical characteristics, as it will be shown further.

## 2.2 Properties of the interpolating functions

Let us define the vector  $\vec{\Phi}_i$  associated to the interpolating function  $\Phi_i(t)$  as:

$$\vec{\Phi}_i = \begin{pmatrix} \Phi_i(t_0) \\ \vdots \\ \Phi_i(t_{N-1}) \end{pmatrix}. \quad (4)$$

It is then possible to build the matrix  $[\Phi]$ :

$$[\Phi] = \begin{pmatrix} \vec{\Phi}_0 & \vec{\Phi}_1 & \vec{\Phi}_2 \end{pmatrix} = \begin{pmatrix} \Phi_0(t_0) & \Phi_1(t_0) & \Phi_2(t_0) \\ \vdots & \vdots & \vdots \\ \Phi_0(t_{N-1}) & \Phi_1(t_{N-1}) & \Phi_2(t_{N-1}) \end{pmatrix}. \quad (5)$$

One of the main properties of the Tchebychev polynomials lies in the orthonormality of the vectors associated to these interpolating functions:

$$[\Phi]^T[\Phi] = [I_3] \quad (6)$$

where  $[I_3]$  is the unit matrix ( $3 \times 3$ ).

### 2.3 Estimation of the parameters $\{P_0, P_1, P_2\}$

Let us define the vector  $\vec{X}$  as:

$$\vec{X} = \begin{pmatrix} x(t_0) \\ \vdots \\ x(t_{N-1}) \end{pmatrix}. \quad (7)$$

This vector may be modeled by:

$$\vec{X} = [\Phi]\vec{P} + \vec{E} \quad (8)$$

where  $\vec{P}$  is the vector whose components are the three parameters we want to estimate, and  $\vec{E}$  the vector standing for the purely random part of  $\vec{X}$ :

$$\vec{P} = \begin{pmatrix} P_0 \\ P_1 \\ P_2 \end{pmatrix} \quad \text{and} \quad \vec{E} = \begin{pmatrix} e(t_0) \\ \vdots \\ e(t_{N-1}) \end{pmatrix}. \quad (9)$$

In order to estimate  $\vec{P}$ , we have to calculate:

$$[\Phi]^T \vec{X} = [\Phi]^T [\Phi]\vec{P} + [\Phi]^T \vec{E}. \quad (10)$$

From equation (6) and because the ensemble average  $\langle [\Phi]^T \vec{E} \rangle = 0$ , it is possible to estimate  $\vec{P}$  with  $\tilde{P}$  defined by:

$$\tilde{P} = [\Phi]^T \vec{X}. \quad (11)$$

Thus, the estimate  $\hat{P}_j$  of the parameter  $P_j$  is easily obtained by calculating:

$$\hat{P}_j = \vec{\Phi}_j^T \cdot \vec{X} = \sum_{i=0}^{N-1} \Phi_j(t_i) x(t_i). \quad (12)$$

### 2.4 Relationships between $\{C_0, C_1, C_2\}$ and $\{P_0, P_1, P_2\}$

The classical parameters  $\{C_0, C_1, C_2\}$  of (1) may be easily deduced from the parameters  $\{P_0, P_1, P_2\}$  of (3). It may be noticed that, with an infinite precision calculation, the following relationships are absolutely rigorous:

the only differences must be attributed to truncature errors. Moreover, the Tchebychev polynomials minimize this sort of errors, because their covariance matrix is optimized for avoiding bad conditioning problems.

$$C_0 = \frac{1}{\sqrt{N}}P_0 - \sqrt{\frac{3(N-1)}{N(N+1)}}P_1 + \sqrt{\frac{5(N-2)(N-1)}{N(N+1)(N+2)}}P_2. \quad (13)$$

$C_0$ , as  $P_0$ ,  $P_1$  and  $P_2$ , has the dimension of a time.

$$C_1 = \frac{2}{\tau_0}\sqrt{\frac{3}{(N-1)N(N+1)}}P_1 - \frac{6}{\tau_0}\sqrt{\frac{5(N-1)}{(N-2)N(N+1)(N+2)}}P_2. \quad (14)$$

$C_1$ , as  $\frac{P_1}{\tau_0}$  and  $\frac{P_2}{\tau_0}$ , is dimensionless.

$$C_2 = \frac{6}{\tau_0^2}\sqrt{\frac{5}{(N-2)(N-1)N(N+1)(N+2)}}P_2. \quad (15)$$

$C_2$ , as  $\frac{P_2}{\tau_0^2}$ , has the dimension of a frequency.

## 2.5 The moment condition

It is important to know if the estimates  $\hat{P}_i$  will converge, or, and this is equivalent, if the variance  $\langle \hat{P}_i^2 \rangle$  is finite.

It may be demonstrated that such a variance may be calculated in the frequency domain (see [9] and Appendix 1) as:

$$\langle \hat{P}_i^2 \rangle = \int_{-\infty}^{+\infty} |\varphi_i(f)|^2 S_x^{2S}(f) df \quad (16)$$

where  $\varphi_i(f)$  is the Fourier transform of the interpolating function  $\Phi_i(t)$  and  $S_x^{2S}(f)$  is the two-sided power spectral density of  $x(t)$ , see (26).

We assume that  $S_x^{2S}(f)$  is modeled by a power law with a negative or null exponent (see (29)):  $S_x^{2S}(f) \propto f^\alpha$ . The convergence condition for the estimates  $\hat{P}_i$  is then:

$$\int_{-\infty}^{+\infty} |\varphi_i(f)|^2 f^\alpha df \quad \text{converges.} \quad (17)$$

The **moment condition** (see [7] and Appendix 2) implies the following equivalence:

$$\int_{-\infty}^{+\infty} |\varphi_i(f)|^2 f^\alpha df \quad \text{converges} \quad \Leftrightarrow \quad \sum_{j=0}^{N-1} \Phi_i(t_j) t_j^q = 0 \quad \text{for} \quad 0 \leq q \leq \frac{-\alpha - 1}{2}. \quad (18)$$

Moreover, since the Tchebychev polynomials constitute an orthonormal basis, each  $q$ -order polynomial may be rewritten as a linear combination of the Tchebychev polynomials  $\Phi_i(t)$  whose order is smaller or equal to  $q$ :

$$t^q = \sum_{i=0}^q P_i \Phi_i(t). \quad (19)$$

Consequently, the polynomial  $t^q$  is orthogonal to all Tchebychev polynomials whose order is greater than  $q$ :

$$\sum_{j=0}^{N-1} \Phi_i(t_j) t_j^q = 0 \quad \text{if and only if } i > q. \quad (20)$$

This yields a simple method for verifying the convergence of an estimate  $\hat{P}_i$  for a given power law model of  $S_x^{2S}(f)$ .

As an example, let us consider that  $S_x^{2S}(f)$  may be modeled by a  $f^{-4}$  power law (i. e. a random walk FM).

The condition (18) implies that the variance of the estimator  $P_i$  will be finite if and only if :

$$\sum_{j=0}^{N-1} \Phi_i(t_j) t_j^q = 0 \quad \text{for } q = 0 \quad \mathbf{and} \quad q = 1. \quad (21)$$

According to the properties of the orthogonal polynomials (20), only  $\Phi_2(t)$  satisfies the condition (21). This means that the variance of the parameters  $P_0$  and  $P_1$  is infinite unless we use a low cut-off frequency  $f_l$ .

In other words, the divergence effect of such a noise for the lowest frequencies induces a linear drift: the lower the low cut-off frequency, the higher the variance of the coefficients of this drift. Therefore, in order to ensure the convergence of such a noise, we just have to remove a linear drift from the data sequence.

It may be noticed that this moment condition is much more useful than this application. It is the condition which allows us to identify the convergence for low frequency noises and for high order drifts. It may be applied to create new estimators (new variances) or to simulate low frequency noises with a very low cut-off frequency  $f_l$ .

Table 1 summarizes the convergences properties from  $f^{-4}$  noise to white noise.

[Table 1 about here.]

### 3 Assessment principle of the interpolation and extrapolation errors

#### 3.1 Estimation of the residuals

From (11), the residuals may be defined as a vector  $\vec{\varrho}$ :

$$\vec{\varrho} = \vec{X} - [\Phi]\vec{P}. \quad (22)$$

The variance of the residuals  $\sigma_e^2$  may be estimated by:

$$\sigma_e^2 = \frac{1}{N} \langle \vec{\varrho}^T \cdot \vec{\varrho} \rangle. \quad (23)$$

From (22) and because the ensemble average  $\langle \vec{\varrho}^T [\Phi]\vec{P} \rangle = 0$ :

$$\langle \vec{\varrho}^T \cdot \vec{\varrho} \rangle = \langle \vec{X}^T \vec{X} \rangle - \langle \vec{P}^T \vec{P} \rangle. \quad (24)$$

The scalar product  $\langle \vec{X}^T \vec{X} \rangle$  is  $N$  times the variance  $\sigma_X^2$  of the  $x(t)$  data and the scalar product  $\langle \vec{P}^T \vec{P} \rangle$  is the sum of the variances of each estimate  $\hat{P}_0$ ,  $\hat{P}_1$  and  $\hat{P}_2$ . Then, the variance of the residuals may be estimated by:

$$\sigma_e^2 = \sigma_X^2 - \frac{1}{N} (\sigma_{P_0}^2 + \sigma_{P_1}^2 + \sigma_{P_2}^2). \quad (25)$$

#### 3.2 Correlation of the samples

Obviously, the long term behavior of the TIE depends greatly on the type of noise. The autocorrelation function  $R_x(t)$  of the  $x(t)$  data contains the information about this type of noise. The power spectral density (PSD)  $S_x(f)$  is the Fourier Transform of the autocorrelation function  $R_x(t)$ . Thus, denoting by  $S_x^{2S}(f)$  the two-sided PSD and  $S_x(f)$  the one-sided PSD defined as :

$$\begin{cases} S_x(f) = 2S_x^{2S}(f) & \text{if } f \geq 0 \\ S_x(f) = 0 & \text{if } f < 0 \end{cases} \quad (26)$$

we have:

$$\begin{aligned} R_x(t_j - t_i) = \langle x(t_i) \cdot x(t_j) \rangle &= \int_{-\infty}^{+\infty} S_x^{2S}(f) e^{+j2\pi f(t_j - t_i)} df \\ &= \int_0^{+\infty} S_x(f) \cos [2\pi f(t_j - t_i)] df. \end{aligned} \quad (27)$$

Taking into account  $f_l$ , the low cut-off frequency and  $f_h$ , the high cut-off frequency, (27) may be rewritten:

$$R_x(t_j - t_i) = \int_{f_l}^{f_h} S_x(f) \cos [2\pi f(t_j - t_i)] df. \quad (28)$$

We will use the power law model of  $S_x(f)$ :

$$S_x(f) = \sum_{\alpha=-4}^0 k_\alpha f^\alpha. \quad (29)$$

It may be noticed that this model is more generally expressed in terms of frequency noise with the power spectral density  $S_y(f)$  of the frequency deviation  $y(t)$ . Since  $y(t)$  is defined as:

$$y(t) = \frac{dx(t)}{dt}, \quad (30)$$

its power spectral density is then linked to  $S_x(f)$  by:

$$S_y(f) = 4\pi^2 f^2 S_x(f). \quad (31)$$

The power law model (29) may be rewritten:

$$S_y(f) = \sum_{\alpha=-2}^{+2} h_\alpha f^\alpha \quad (32)$$

where the noise levels  $h_\alpha$  are linked to the  $k_\alpha$  by:

$$h_\alpha = 4\pi^2 k_{\alpha-2}. \quad (33)$$

In the following, the different types of noise are called:

- **white PM** for  $\alpha = 0$  (PM stands for Phase Modulation),
- **flicker PM** for  $\alpha = -1$ ,
- **white FM** for  $\alpha = -2$  (FM stands for Frequency Modulation),
- **flicker FM** for  $\alpha = -3$ ,
- **random walk FM** for  $\alpha = -4$ .

### 3.3 Calculation method of the TIE

By hypothesis, we consider that the TIE is the difference between the true time deviation  $x(t)$  at time  $t$ , and the extrapolation of the parabola (previously estimated from  $t_0$  to  $t_{N-1}$ ) up to this time  $t > t_{N-1}$ :

$$\text{TIE}(t) = x(t) - \hat{P}_0 \Phi_0(t) - \hat{P}_1 \Phi_1(t) - \hat{P}_2 \Phi_2(t) \quad \text{and} \quad t > t_{N-1}. \quad (34)$$

Thus, the quadratic ensemble average of TIE may be estimated by:

$$\begin{aligned} \langle \text{TIE}^2(t) \rangle &= \langle x^2(t) \rangle + \langle \hat{P}_0^2 \rangle \Phi_0^2(t) + \langle \hat{P}_1^2 \rangle \Phi_1^2(t) + \langle \hat{P}_2^2 \rangle \Phi_2^2(t) \\ &\quad - 2 \left[ \langle x(t) \hat{P}_0 \rangle \Phi_0(t) + \langle x(t) \hat{P}_1 \rangle \Phi_1(t) + \langle x(t) \hat{P}_2 \rangle \Phi_2(t) \right] \\ &\quad + 2 \left[ \langle \hat{P}_0 \hat{P}_1 \rangle \Phi_0(t) \Phi_1(t) + \langle \hat{P}_0 \hat{P}_2 \rangle \Phi_0(t) \Phi_2(t) + \langle \hat{P}_1 \hat{P}_2 \rangle \Phi_1(t) \Phi_2(t) \right]. \end{aligned} \quad (35)$$

Consequently, for each type of noise, we have to know:

- $\langle x^2(t) \rangle = R_x(t)$ , the autocorrelation function of  $x(t)$  ;
- the 3 variances  $\langle \hat{P}_i^2 \rangle = \sigma_{P_i}^2$  ;
- the 3 covariances  $\langle \hat{P}_i \hat{P}_j \rangle = \text{Cov}(P_i, P_j)$ : actually, only  $\langle \hat{P}_0 \hat{P}_2 \rangle \neq 0$ ;
- the 3 covariances  $\langle x(t) \hat{P}_i \rangle = \text{Cov}(x(t), P_i)$ .

### 3.4 Example of the white PM noise

We illustrate the calculation of the TIE with the case of white PM.

- Autocorrelation (see table 2):

$$R_x(t) = \sigma_x^2 \delta(t) = k_0 f_h \delta(t), \quad (36)$$

where  $\sigma_x^2$  is the variance of the  $x(t)$  data,  $k_0$  is the white PM noise level and  $f_h$  is the low cut-off frequency of the system.

- Variances and covariances of the parameters  $\hat{P}_i$ : we define  $[C_v]$  the matrix of the parameter covariances by:

$$[C_v] = \left\langle \vec{\hat{P}} \cdot \vec{\hat{P}}^T \right\rangle = \left\langle [\Phi]^T \vec{X} \cdot \vec{X}^T [\Phi] \right\rangle = [\Phi]^T \left\langle \vec{X} \cdot \vec{X}^T \right\rangle [\Phi] \quad (37)$$

where the component  $(i, j)$  of the matrix  $\left\langle \vec{X} \cdot \vec{X}^T \right\rangle$  is:

$$\left\langle \vec{X} \cdot \vec{X}^T \right\rangle_{i,j} = \langle x(t_i)x(t_j) \rangle = R_x(t_j - t_i). \quad (38)$$

Therefore:

$$\left\langle \vec{X} \cdot \vec{X}^T \right\rangle = k_0 f_h [I_N] \quad (39)$$

where  $[I_N]$  is the unit matrix ( $N \times N$ ).

$$[C_v] = k_0 f_h [\Phi]^T [\Phi] = k_0 f_h [I_3]. \quad (40)$$

Thus, in the case of a white PM noise, the use of the interpolating functions  $\Phi_i(t)$  lead us to parameters which are completely decorrelated and with the same variance:

$$\text{Cov}(P_i, P_j) = 0 \quad \text{if } i \neq j \quad \text{and} \quad \sigma_{P_i}^2 = k_0 f_h. \quad (41)$$

- Covariances  $\left\langle x(t)\hat{P}_i \right\rangle$ :

$$\left\langle x(t)\vec{\hat{P}} \right\rangle = \left\langle x(t)[\Phi]^T \vec{X} \right\rangle = [\Phi]^T \left\langle x(t)\vec{X} \right\rangle. \quad (42)$$

If  $t > t_{N-1}$

$$\left\langle x(t)\vec{X} \right\rangle = \begin{pmatrix} R_x(t - t_0) \\ \vdots \\ R_x(t - t_{N-1}) \end{pmatrix} = 0. \quad (43)$$

Consequently,  $\text{Cov}(x(t), P_i) = 0$ .

- Variance of the residuals:

$$\sigma_e^2 = R_x(0) - \frac{1}{N} 3k_0 f_h = k_0 f_h \frac{N-3}{N}. \quad (44)$$

The number of samples  $N$  should be at least equal to 100, and we may assume that  $N \gg 1$ . Therefore:

$$\sigma_e^2 \approx k_0 f_h. \quad (45)$$

Thus, the removal of a quadratic drift in a white PM noise does not modify its variance.

- Estimation of the TIE:

$$\langle \text{TIE}^2(t) \rangle = k_0 f_h \left[ 1 + \Phi_0^2(t) + \Phi_1^2(t) + \Phi_2^2(t) \right] \quad (46)$$

$$\begin{aligned} \langle \text{TIE}^2(t) \rangle = & \frac{k_0 f_h}{(N-2)(N-1)N(N+1)(N+2)} \left[ 180 \frac{t^4}{\tau_0^4} - 360(N-1) \frac{t^3}{\tau_0^3} \right. \\ & + 36(7N^2 - 15N + 7) \frac{t^2}{\tau_0^2} - 36(2N^3 - 7N^2 + 7N - 2) \frac{t}{\tau_0} \\ & \left. + (N^5 + 9N^4 - 41N^3 + 51N^2 - 32N + 12) \right]. \end{aligned} \quad (47)$$

One may easily admit that  $N \gg 1$ , then

$$\langle \text{TIE}^2(t) \rangle \approx \frac{k_0 f_h}{N^5} \left( 180 \frac{t^4}{\tau_0^4} - 360N \frac{t^3}{\tau_0^3} + 252N^2 \frac{t^2}{\tau_0^2} - 72N^3 \frac{t}{\tau_0} + N^5 + 9N^4 \right). \quad (48)$$

Let  $T_m$  denote the measurement time, i. e. the duration of the interpolated sequence:

$$T_m = N\tau_0. \quad (49)$$

Equation (48) may be rewritten versus  $T_m$ :

$$\langle \text{TIE}^2(t) \rangle \approx \frac{k_0 f_h}{N} \left( N + 180 \frac{t^4}{T_m^4} - 360 \frac{t^3}{T_m^3} + 252 \frac{t^2}{T_m^2} - 72 \frac{t}{T_m} + 9 \right). \quad (50)$$

Since the origin of the time  $t$  is the beginning of the interpolated sequence,  $t$  must be greater than  $T_m$ .

This argument  $t$  may be replaced by the prediction time  $T_p$ .  $T_p$  is the extrapolation time whose origin is the beginning of the extrapolated sequence (and the end of the interpolated sequence).  $T_p$  is then linked to the argument  $t$  of (50) by:

$$t = T_m + T_p. \quad (51)$$

By using (51), (50) becomes the following function of the two variables  $T_m$  and  $T_p$ :

$$\langle \text{TIE}^2(T_m, T_p) \rangle \approx \frac{k_0 f_h}{N} \left( N + 180 \frac{T_p^4}{T_m^4} + 360 \frac{T_p^3}{T_m^3} + 252 \frac{T_p^2}{T_m^2} + 72 \frac{T_p}{T_m} + 9 \right). \quad (52)$$

## 4 Theoretical results

Only the final results are given here, but the calculation details are available upon request to the authors.

### 4.1 Preliminary calculation

#### 4.1.1 Autocorrelation of a time deviation sequence

The results given in Table 2 were calculated from (28).

[Table 2 about here.]

Since we are interested in the long term behavior of clocks, we will limit this study to the 3 “redest” frequency noises: white FM, flicker FM and random walk FM.

#### 4.1.2 Variance of the parameters $P_1$ and $P_2$

According to the moment condition (18), the variance of the parameter  $P_0$  diverges for white FM, flicker FM and random walk FM (see Table 1). On the same hand, the variance of the parameter  $P_1$  diverges for flicker FM and random walk FM.

- White FM:

$$\sigma_{P_1}^2 \approx \frac{\pi^2 N^2 k_{-2} \tau_0}{5}. \quad (53)$$

$$\sigma_{P_2}^2 \approx \frac{\pi^2 N^2 k_{-2} \tau_0}{21}. \quad (54)$$

- Flicker FM:

$$\sigma_{P_2}^2 \approx \frac{5\pi^2 N^3 k_{-3} \tau_0^2}{72}. \quad (55)$$

- Random walk FM:

$$\sigma_{P_2}^2 \approx \frac{\pi^4 N^4 k_{-4} \tau_0^3}{63}. \quad (56)$$

All the above equations were obtained under the assumption  $N \gg 1$ .

## 4.2 Case of a quadratic interpolation

### 4.2.1 Variance of the residuals

From (25) we got the following results versus  $T_m = N\tau_0$ :

- White FM :

$$\sigma_e^2(T_m) \approx \frac{3\pi^2 k_{-2} T_m}{35}. \quad (57)$$

- Flicker FM:

$$\sigma_e^2(T_m) \approx \frac{\pi^2 k_{-3} T_m^2}{24}. \quad (58)$$

- Random walk FM:

$$\sigma_e^2(T_m) \approx \frac{\pi^4 k_{-4} T_m^3}{315}. \quad (59)$$

All the above equations were obtained under the assumption  $N \gg 1$ , i. e.  $T_m \gg \tau_0$ .

### 4.2.2 Estimation of the TIE using the noise levels

The theoretical calculation of (35) yields the following variances versus the measurement time  $T_m$  and the prediction time  $T_p$  (see definitions of  $T_m$  in (49) and  $T_p$  in (51)):

- White FM:

$$\langle \text{TIE}^2(T_m, T_p) \rangle \approx \frac{6\pi^2 k_{-2} T_m}{35} \left( 50 \frac{T_p^4}{T_m^4} + 100 \frac{T_p^3}{T_m^3} + 69 \frac{T_p^2}{T_m^2} + 19 \frac{T_p}{T_m} + 1 \right). \quad (60)$$

- Flicker FM:

$$\begin{aligned} \langle \text{TIE}^2(T_m, T_p) \rangle \approx & \frac{\pi^2 k_{-3} T_m^2}{8} \left[ 192 \frac{T_p^6}{T_m^6} + 576 \frac{T_p^5}{T_m^5} + 692 \frac{T_p^4}{T_m^4} + 424 \frac{T_p^3}{T_m^3} + 136 \frac{T_p^2}{T_m^2} + 20 \frac{T_p}{T_m} + 1 \right. \\ & \left. + 96 \frac{T_p^3}{T_m^3} \ln \left( \frac{T_p}{T_m + T_p} \right) \left( 2 \frac{T_p^4}{T_m^4} + 7 \frac{T_p^3}{T_m^3} + 9 \frac{T_p^2}{T_m^2} + 5 \frac{T_p}{T_m} + 1 \right) \right]. \quad (61) \end{aligned}$$

- Random walk FM:

$$\langle \text{TIE}^2(T_m, T_p) \rangle \approx \frac{2\pi^4 k_{-4} T_m^3}{315} \left( 450 \frac{T_p^4}{T_m^4} + 690 \frac{T_p^3}{T_m^3} + 303 \frac{T_p^2}{T_m^2} + 42 \frac{T_p}{T_m} + 2 \right). \quad (62)$$

All the above equations were obtained under the assumption  $N \gg 1$ . Thus, under this assumption, the dependence versus  $N$  cancels out: the variance of the residuals only depends on the length of the interpolated sequence  $T_m$ , and the variance of the TIE only depends on the ratio  $\frac{T_p}{T_m}$ , whatever the number of samples  $N$  is.

#### 4.2.3 Estimation of the TIE using the variance of the residuals

The relationships (60) to (62) needs an explicit knowledge of the noise levels  $k_\alpha$ . However, for very long term interpolation (several days), we may be sure of the dominant type of noise: the flicker FM for a cesium clock or the random walk FM for a quartz oscillator.

Thus, the variance of the TIE may be directly estimated from the variance of the residuals :

- White FM : from (60) and (57) we got:

$$\langle \text{TIE}^2(T_m, T_p) \rangle \approx 2\sigma_e^2 \left( 50 \frac{T_p^4}{T_m^4} + 100 \frac{T_p^3}{T_m^3} + 69 \frac{T_p^2}{T_m^2} + 19 \frac{T_p}{T_m} + 1 \right). \quad (63)$$

- Flicker FM: from (61) and (58) we got:

$$\begin{aligned} \langle \text{TIE}^2(T_m, T_p) \rangle \approx & 3\sigma_e^2 \left[ 192 \frac{T_p^6}{T_m^6} + 576 \frac{T_p^5}{T_m^5} + 692 \frac{T_p^4}{T_m^4} + 424 \frac{T_p^3}{T_m^3} + 136 \frac{T_p^2}{T_m^2} + 20 \frac{T_p}{T_m} + 1 \right. \\ & \left. + 96 \frac{T_p^3}{T_m^3} \ln \left( \frac{T_p}{T_m + T_p} \right) \left( 2 \frac{T_p^4}{T_m^4} + 7 \frac{T_p^3}{T_m^3} + 9 \frac{T_p^2}{T_m^2} + 5 \frac{T_p}{T_m} + 1 \right) \right]. \quad (64) \end{aligned}$$

- Random walk FM: from (62) and (59) we got:

$$\langle \text{TIE}^2(T_m, T_p) \rangle \approx 2\sigma_e^2 \left( 450 \frac{T_p^4}{T_m^4} + 690 \frac{T_p^3}{T_m^3} + 303 \frac{T_p^2}{T_m^2} + 42 \frac{T_p}{T_m} + 2 \right). \quad (65)$$

However, such a method is less precise than the use of a correct estimation of the noise levels. This is due to the statistics of the estimate of the variance of the residuals (see section 6).

#### 4.2.4 Asymptotic behavior

If  $\frac{T_p}{T_m} \gg 1$ , i. e. if  $T_p \gg T_m$ :

- White FM:

$$\lim_{T_p \rightarrow \infty} \langle \text{TIE}^2(T_m, T_p) \rangle \approx 100 \sigma_e^2 \frac{T_p^4}{T_m^4}. \quad (66)$$

- Flicker FM:

$$\lim_{T_p \rightarrow \infty} \langle \text{TIE}^2(T_m, T_p) \rangle \approx 300 \sigma_e^2 \frac{T_p^4}{T_m^4}. \quad (67)$$

- Random walk FM:

$$\lim_{T_p \rightarrow \infty} \langle \text{TIE}^2(T_m, T_p) \rangle \approx 900 \sigma_e^2 \frac{T_p^4}{T_m^4}. \quad (68)$$

It may be noticed that, for a fixed value of  $\sigma_e^2$ , the asymptotic ratio of equation (68) over equation (67) as well as the asymptotic ratio of equation (67) over equation (66) is exactly equal to 3 when  $T_p$  tends toward infinity.

Moreover, for long  $T_p$  values, the main contribution of the TIE is obviously due to the error on the quadratic parameter  $P_2$ . Using a classical quadratic model such as (1), the variance of the TIE should be linked to the variance of the quadratic classical parameter  $C_2$  by:

$$\lim_{T_p \rightarrow \infty} \langle \text{TIE}^2(T_m, T_p) \rangle \approx \sigma_{C_2}^2 T_p^4. \quad (69)$$

Using (15), the variance of the quadratic classical parameter  $C_2$  may be obtained from the variance of the quadratic Tchebychev parameter  $P_2$ :

$$\sigma_{C_2}^2 \approx \frac{180}{N^5 \tau_0^4} \sigma_{P_2}^2 = \frac{180}{N T_m} \sigma_{P_2}^2. \quad (70)$$

It is easy to verify that (69) gives the same results as (66), (67) and (68).

### 4.3 Case of a linear interpolation

Cesium clocks are not affected by a quadratic drift. If such clocks are used, we may limit the fit to a linear interpolation. In this case, for long term, the main contribution to the TIE will be due to the error on the

parameter  $P_1$  and then will be lower than for a quadratic interpolation. It is then strongly recommended to extrapolate the time deviation of a Cesium clock from a linear fit. On the other hand, the variance of the residuals will be higher because a quadratic adjustment remains closer to the time data than a linear one.

#### 4.3.1 Variance of the residuals

- White FM:

$$\sigma_e^2(T_m) \approx \frac{2\pi^2 k_{-2} T_m}{15} \quad (71)$$

- Flicker FM:

$$\sigma_e^2(T_m) \approx \frac{\pi^2 k_{-3} T_m^2}{9} \quad (72)$$

- Random walk FM<sup>3</sup>:

$$\sigma_e^2(T_m) \approx \frac{2\pi^4 k_{-4} T_m^3}{105} \quad (73)$$

All the above equations were obtained under the assumption  $N \gg 1$ , i. e.  $T_m \gg \tau_0$ .

#### 4.3.2 Estimation of the TIE using the noise levels

- White FM:

$$\langle \text{TIE}^2(T_m, T_p) \rangle \approx \frac{4\pi^2 k_{-2} T_m}{15} \left( 9 \frac{T_p^2}{T_m^2} + 9 \frac{T_p}{T_m} + 1 \right). \quad (74)$$

- Flicker FM:

$$\begin{aligned} \langle \text{TIE}^2(T_m, T_p) \rangle \approx & \frac{\pi^2 k_{-3} T_m^2}{3} \left[ 12 \frac{T_p^4}{T_m^4} + 24 \frac{T_p^3}{T_m^3} + 20 \frac{T_p^2}{T_m^2} + 8 \frac{T_p}{T_m} + 1 \right. \\ & + 2 \ln \left( 1 + \frac{T_p}{T_m} \right) \left( 6 \frac{T_p^2}{T_m^2} + 6 \frac{T_p}{T_m} + 1 \right) \\ & \left. + 2 \frac{T_p^3}{T_m^3} \ln \left( \frac{T_p}{T_m + T_p} \right) \left( 6 \frac{T_p^2}{T_m^2} + 15 \frac{T_p}{T_m} + 8 \right) \right]. \quad (75) \end{aligned}$$

---

<sup>3</sup>The random walk FM is treated here for homogeneity, but a Cesium clock is never affected by this type of noise.

- Random walk FM<sup>3</sup>:

$$\langle \text{TIE}^2(T_m, T_p) \rangle \approx \frac{8\pi^4 k_{-4} T_m^3}{105} \left( 35 \frac{T_p^3}{T_m^3} + 39 \frac{T_p^2}{T_m^2} + 11 \frac{T_p}{T_m} + 1 \right). \quad (76)$$

All the above equations were obtained under the assumption  $N \gg 1$ , i.e.  $T_m \gg \tau_0$ .

### 4.3.3 Estimation of the TIE using the variance of the residuals

From (71), (72), (73) and (74), (75), (76), we obtained:

- White FM:

$$\langle \text{TIE}^2(T_m, T_p) \rangle \approx 2\sigma_e^2 \left( 9 \frac{T_p^2}{T_m^2} + 9 \frac{T_p}{T_m} + 1 \right). \quad (77)$$

- Flicker FM:

$$\begin{aligned} \langle \text{TIE}^2(T_m, T_p) \rangle \approx & 3\sigma_e^2 \left[ 12 \frac{T_p^4}{T_m^4} + 24 \frac{T_p^3}{T_m^3} + 20 \frac{T_p^2}{T_m^2} + 8 \frac{T_p}{T_m} + 1 \right. \\ & + 2 \ln \left( 1 + \frac{T_p}{T_m} \right) \left( 6 \frac{T_p^2}{T_m^2} + 6 \frac{T_p}{T_m} + 1 \right) \\ & \left. + 2 \frac{T_p^3}{T_m^3} \ln \left( \frac{T_p}{T_m + T_p} \right) \left( 6 \frac{T_p^2}{T_m^2} + 15 \frac{T_p}{T_m} + 8 \right) \right]. \quad (78) \end{aligned}$$

- Random walk FM<sup>3</sup>:

$$\langle \text{TIE}^2(T_m, T_p) \rangle \approx 4\sigma_e^2 \left( 35 \frac{T_p^3}{T_m^3} + 39 \frac{T_p^2}{T_m^2} + 11 \frac{T_p}{T_m} + 1 \right). \quad (79)$$

### 4.3.4 Asymptotic behavior

If  $\frac{t}{\tau_0} \gg N$ , i. e. if  $t \gg T_m$ :

- White FM:

$$\lim_{T_p \rightarrow \infty} \langle \text{TIE}^2(T_m, T_p) \rangle \approx 18\sigma_e^2 \frac{T_p^2}{T_m^2}. \quad (80)$$

- Flicker FM:

$$\lim_{T_p \rightarrow \infty} \langle \text{TIE}^2(T_m, T_p) \rangle \approx 36\sigma_e^2 \frac{T_p^2}{T_m^2} \ln \left( \frac{T_p}{T_m} \right). \quad (81)$$

- Random walk FM<sup>3</sup>:

$$\lim_{T_p \rightarrow \infty} \langle \text{TIE}^2(T_m, T_p) \rangle \approx 140 \sigma_e^2 \frac{T_p^3}{T_m^3} \quad (82)$$

In this case, the time dependences of the variance of the TIE are different for the 3 types of noise:  $T_p^2/T_m^2$  for the white FM,  $\ln(T_p/T_m)T_p^2/T_m^2$  for the flicker FM and  $T_p^3/T_m^3$  for the random walk FM. This is due to the divergence of the variance of  $P_1$  for flicker and random walk FM.

[Table 3 about here.]

#### 4.4 Relationships with the Time Variance

The Time Variance (TVAR), and its square root, the Time Deviation (TDEV), are commonly used for time analysis [10]. Table 4 gives the relationships between the variance of the residuals  $\sigma_e^2$  and  $\text{TVAR}(\tau)$  for an integration time  $\tau = T_m = N\tau_0$ . It is interesting to notice that, for a given type of noise, the ratio  $\sigma_e^2/\text{TVAR}(\tau)$  is constant.

[Table 4 about here.]

## 5 Experimental validation

### 5.1 Monte-Carlo simulations

In order to verify the equations (60) to (62) and (74) to (76), we simulated time deviation sequences of different types of noise (white FM, flicker FM and random walk FM) and we used quadratic and linear fits. For each type of noise, 10,000 realizations were calculated with

- the same noise level:  $k_{-2} = 1.4 \times 10^{-4}\text{s}$ ,  $k_{-3} = 3.3 \times 10^{-8}$  or  $k_{-4} = 5.0 \times 10^{-12}\text{s}^{-1}$  for the quadratic fit,  $k_{-2} = 3.5 \times 10^{-3}\text{s}$ ,  $k_{-3} = 4.8 \times 10^{-7}$  or  $k_{-4} = 3.3 \times 10^{-11}\text{s}^{-1}$  for the linear fit,
- the same number of data: 65,536,

- the same number of data taken into account for the fit:  $N = 8640$ ,
- the same time of estimation of the TIE:  $\frac{T_m + T_p}{\tau_0}$  equals to  $\{8640, 9900, 11350, 13000, 14900, 17000, 19500, 22400, 25700, 29400, 33700, 38600, 44300, 50700, 58100, 65535\}$ .

The noise levels were chosen for getting a variance of the residuals equal to 1.

[Figure 4 about here.]

Figure 4 shows the curves corresponding to the square root of equations (60) to (62) compared to the standard deviation estimated from the 10,000 simulations (i.e. half the width of the Gaussian of figure 2). The simulations exhibits a quite good agreement with the theoretical curves.

The asymptotic behaviors are reached at the end of the log-log graphs. The benefits of the linear interpolation are obvious.

## 5.2 Real clocks (quartz USO and atomic clocks)

[Figure 5 about here.]

[Figure 6 about here.]

Figure 5 compares the long term behavior of a real ultra-stable quartz oscillator (denoted “quartz 1” in table 5) to the bounds given by the estimated standard deviation of the TIE (the square root of equations (60) to (62)).

The data from the oscillator are time deviations sampled with a sampling period  $\tau_0 = 10$  s, obtained at CNES Toulouse (France) with their own reference clocks (Cs HP 5071A option 001 and H-Maser EFOS-16). The fit was carried out over the first 24 hours of the sequence and extrapolated over the whole sequence (90 hours).

Allan variance revealed that 2 types of noise must be taken into account: white FM ( $h_0 = 10^{-22}$  s, i.e.  $k_{-2} = 2,5 \times 10^{-24}$  s) and random walk FM ( $h_{-2} = 1,5 \times 10^{-31}$  s<sup>-1</sup>, i.e.  $k_{-4} = 4 \times 10^{-33}$  s<sup>-1</sup>). Thus, the bounds of figures 5 were obtained by using the square root of the sum of (60) and (62).

In figure 6, the fit was still performed over a 24 hours sequence, but the interpolated sequence was shifted along the 90 hours data sequence. At each step ( $\tau_0 = 10\text{s}$ ) of this shift, the fit was extrapolated over 3.5 hours. The TIE measured at this instant ( $T_p = 3.5$  hours) was plotted (solid line) and the interpolated sequence was shifted again.

The TIE bounds of the upper figure (dashed lines) were estimated from the noise levels as in figure 5. In the lower figure, the TIE bounds were estimated from the variance of the residuals, which was calculated at each step of the shift. In this case, we assumed that the random walk FM was dominant and we used the square root of (65).

The experimental TIE curves remain generally in the theoretical bounds. The few moments where the TIE is outside the bounds is fully compatible with the statistics of TIE (see section 6).

[Table 5 about here.]

[Table 6 about here.]

Table 5 shows experimental results obtained with several clocks and a quadratic interpolation. The noise levels were estimated from Allan variance measurements. This table compares “ $\sigma_e$  exp.”, the standard deviation of the residuals, with “ $\sigma_e$  theo.”, the estimate of  $\sigma_e$  obtained from the square root of (57), (58), (59) and the noise level coefficients.

This table compares also “ $\sigma_{TIE}$  exp.”, the measured error between the parabola extrapolated over 3.5 hours and the real time deviation of the clock at this instant, with “ $\sigma_{TIE}$  theo. (from  $k_\alpha$ )” estimated from the square root of (60), (61), (62), and with “ $\sigma_{TIE}$  theo. (from  $\sigma_e$ )” estimated from the square root of (63), (64), (65).

Table 6 shows the same type of results but limited to the cesium clocks and with a linear interpolation.

Here also, the agreement between measurements and estimates is quite good.

On the other hand, table 5 and 6 confirm that the standard deviation of the residuals is higher for a linear interpolation than for a quadratic one, whereas it is the opposite for the standard deviation of the TIE.

## 6 Confidence intervals for the interpolation and extrapolation errors

Figures 5 and 6 shows that the real TIE may be outside the bounds of the estimated  $\hat{\sigma}_{TIE}$ . Thus, it is important to know the probability for the real TIE to be inside or outside these bounds. Moreover, it may be useful to improve the TIE bounds by using confidence intervals. This may be achieved by studying the statistics of the TIE.

### 6.1 Statistics of the TIE

As we pointed out in section 1, the real TIE is a centered Gaussian process:

$$\text{TIE}(T_m, T_p) \equiv LG(0, \sigma_{TIE}). \quad (83)$$

where  $LG(m, s)$  denotes a Laplace-Gauss distribution with a mean value  $m$  and a standard deviation  $s$ .

The real  $\sigma_{TIE}$  is estimated by  $\hat{\sigma}_{TIE}$ :

$$\hat{\sigma}_{TIE} = \sqrt{\langle \text{TIE}^2(T_m, T_p) \rangle}. \quad (84)$$

We want to obtain a coefficient  $c_\beta$  ensuring the following confidence interval:

$$-c_\beta \cdot \hat{\sigma}_{TIE} < \text{TIE}(T_m, T_p) < +c_\beta \cdot \hat{\sigma}_{TIE} \quad \text{with } \beta\% \text{ of confidence.} \quad (85)$$

Whatever the values of  $\text{TIE}(T_m, T_p)$  and  $\hat{\sigma}_{TIE}$  are, it is always possible to define a coefficient  $c$  by:

$$\text{TIE}(T_m, T_p) = c \cdot \hat{\sigma}_{TIE}. \quad (86)$$

This coefficient  $c$  may be written as:

$$c = \frac{\text{TIE}(T_m, T_p)}{\hat{\sigma}_{TIE}} = \frac{\text{TIE}(T_m, T_p)}{\sqrt{\langle \text{TIE}^2(T_m, T_p) \rangle}}. \quad (87)$$

The distribution of  $\text{TIE}(T_m, T_p)$  may be considered as a centered Laplace-Gauss distribution with a unitary standard deviation, multiplied by its real standard deviation  $\sigma_{TIE}$  :

$$\text{TIE}(T_m, T_p) \equiv \sigma_{TIE} LG(0, 1). \quad (88)$$

Therefore,  $\langle \text{TIE}^2(T_m, T_p) \rangle$  is  $\chi^2$  distributed with  $\nu$  degrees of freedom (depending on the type of noise) and with a mean value equal to the real variance  $\sigma_{TIE}^2$ :

$$\langle \text{TIE}^2(T_m, T_p) \rangle \equiv \sigma_{TIE}^2 \frac{\chi_\nu^2}{\nu}. \quad (89)$$

Thus, the distribution of the coefficient  $c$  is:

$$c \equiv \frac{\sigma_{TIE} LG(0, 1)}{\sqrt{\sigma_{TIE}^2 \chi_\nu^2 / \nu}} = \frac{LG(0, 1)}{\sqrt{\chi_\nu^2 / \nu}}. \quad (90)$$

By definition,  $c$  follows a Student distribution with  $\nu$  degrees of freedom [11]. Consequently, for building the confidence interval (85), we have to use the Student coefficients for  $c_\beta$ . These coefficients are given in tables [11].

However, it is then necessary to know the number of degrees of freedom of the Student distribution, or, and this is equivalent, the number of degrees of freedom of the  $\chi^2$  distribution followed by  $\langle \text{TIE}^2(T_m, T_p) \rangle$ . Obviously, this number depends on how  $\langle \text{TIE}^2(T_m, T_p) \rangle$  is estimated, i. e. from the variance of the residuals or from the noise levels  $k_\alpha$ .

## 6.2 Estimation from the variance of the residuals

Equations (60) to (62) and (77) to (79) shows that  $\langle \text{TIE}^2(T_m, T_p) \rangle$  is the product of a random variable  $\hat{\sigma}_e^2$  by a constant number. Thus, the distribution of  $\langle \text{TIE}^2(T_m, T_p) \rangle$  is the same as the distribution of  $\hat{\sigma}_e^2$ , i. e. a  $\chi^2$  distribution.

From Monte-Carlo simulations, we observed that the degrees of freedom of the distribution of  $\hat{\sigma}_e^2$  only depend on the type of noise but, curiously, neither on the number of data  $N$ , nor the sampling period  $\tau_0$ .

[Table 7 about here.]

We measured the following degrees of freedom  $\nu$  for the  $\chi^2$  distribution of  $\hat{\sigma}_e^2$ :

- White FM:  $\nu \approx 8$ ;

- Flicker FM:  $\nu \approx 3$ ;
- Random walk FM:  $\nu \approx 2$ .

Therefore, the  $c_\beta$  Student coefficient must be chosen with these degrees of freedom, according to the type of noise. Table 7 gives these coefficients for a 70% confidence interval ( $1\sigma$ ) and for a 95% confidence interval ( $2\sigma$ ).

Figure 7 shows the probability curves of the real TIE to be far from the extrapolated fit for an estimation of  $\hat{\sigma}_{TIE}$  from  $\hat{\sigma}_e^2$ .

[Figure 7 about here.]

### 6.3 Estimation from the noise levels

In this case, the degrees of freedom of  $\langle \text{TIE}^2(T_m, T_p) \rangle$  are equal to the ones of the estimated noise level  $\hat{k}_\alpha$  and then, depend on the accuracy of its estimation. For instance, if  $\hat{k}_\alpha$  was estimated by using the Allan variance, its degrees of freedom depend on the length of the sequence and on the number of sample used by the Allan variance [12, 13]. If this sequence is long enough, the degrees of freedom may be much greater as the values obtained in section 6.2. The degrees of freedom have to be estimated at each noise level measurement [12, 13].

Therefore, if the noise levels are precisely determined, the estimation of  $\hat{\sigma}_{TIE}$  is far better by using this method than from the variance of the residuals.

### 6.4 Example

Let us consider the case of the clock Rb 1 in table 5. Figure 8 displays the Allan variance curve of this clock.

Let us study the case of a 1 day interpolated sequence, and 3.5h prediction time:  $T_m=24\text{h}$  and  $T_p=3.5\text{h}$ .

[Figure 8 about here.]

### 6.4.1 Estimation from the variance of the residuals

Figure 8 shows that the random walk FM is dominant for  $\tau=1\text{day}$  ( $\tau^{1/2}$  slope). From table 7, we can build the following confidence interval:

$$-1.4\hat{\sigma}_{TIE} < \text{TIE}(T_m, T_p) < +1.4\hat{\sigma}_{TIE} \quad \text{with } 70\% \text{ of confidence.} \quad (91)$$

Thus, since the experimental  $\hat{\sigma}_\epsilon$  equals 1.2ns (see table 5), (65) yields for  $T_m=24\text{h}$  and  $t=27.5\text{h}$ :

$$-9.9\text{ns} < \text{TIE}(T_m, T_p) < +9.9\text{ns} \quad \text{with } 70\% \text{ of confidence.} \quad (92)$$

But, for 95% of confidence, we obtain:

$$-4.3\hat{\sigma}_{TIE} < \text{TIE}(T_m, T_p) < +4.3\hat{\sigma}_{TIE} \quad \text{with } 95\% \text{ of confidence} \quad (93)$$

i. e.:

$$-30\text{ns} < \text{TIE}(T_m, T_p) < +30\text{ns} \quad \text{with } 95\% \text{ of confidence.} \quad (94)$$

This huge factor is characteristic of the Student distribution with a low number of degrees of freedom: the probability for having a high estimate is much larger than for a Gaussian process (see fig. 7).

### 6.4.2 Estimation from the noise levels

We will assume that for a 1 day integration time, the random walk FM is dominant and the contributions of the other noises may be neglected. Thus, the noise level  $k_{-4}$  may be estimated from the Allan variance  $\sigma_y^2(1\text{day})$ , by using the following relationship [1, 14]:

$$\sigma_y^2(\tau) = \frac{2\pi^2\tau h_{-2}}{3} = \frac{8\pi^4\tau k_{-4}}{3}. \quad (95)$$

This Allan variance estimate is  $\chi^2$  distributed, and its variance is given by [12]:

$$\sigma^2 \left[ \hat{\sigma}_y^2(\tau) \right] = \left[ \frac{8\pi^4\tau k_{-4}}{3} \right]^2 \frac{9m - 10}{4(m - 1)^2} \quad (96)$$

where the integer  $m$  is the number of independent sub-sequence of  $\tau$ -length in the sequence, i. e. the ratio of the integration time  $\tau$  over the whole sequence length. The number of degrees of freedom of a  $\chi^2$  distribution is [11]:

$$\nu = 2 \frac{\langle \chi^2 \rangle^2}{\sigma^2(\chi^2)}. \quad (97)$$

Thus, from (95), (96) and (97), the number of degrees of freedom of the estimate  $\sigma_y^2(\tau)$  applied to a random walk FM sequence of duration  $m\tau$  is given by:

$$\nu = \frac{8(m-1)^2}{9m-10}. \quad (98)$$

Since the noise level estimate is obtained from this Allan variance estimate, the noise level estimate is  $\chi^2$  distributed with the same number of degrees of freedom as the Allan variance estimate.

- Let us first consider the smallest sequence allowing us the calculation of the Allan variance over one day, i. e. a 2 day length sequence:  $m = 2$ . The first 2 day set of time deviation measurement gives:  $\sigma_y^2(1\text{day}) = 3.9 \times 10^{-25}$ . From this Allan variance estimate, we obtain:  $\hat{k}_{-4} = 1.7 \times 10^{-32}\text{s}^{-1}$ . By using (98), we find  $\nu=1$ . From the table of Student coefficients [11], we can build the following confidence interval:

$$-2\hat{\sigma}_{TIE} < \text{TIE}(T_m, T_p) < +2\hat{\sigma}_{TIE} \quad \text{with } 70\% \text{ of confidence.} \quad (99)$$

For  $T_m=24\text{h}$  and  $T_p=3.5\text{h}$ , (62) yields  $\hat{\sigma}_{TIE}=11\text{ns}$ :

$$-22\text{ns} < \text{TIE}(T_m, T_p) < +22\text{ns} \quad \text{with } 70\% \text{ of confidence.} \quad (100)$$

For 95% of confidence, we obtain:

$$-13\hat{\sigma}_{TIE} < \text{TIE}(T_m, T_p) < +13\hat{\sigma}_{TIE} \quad \text{with } 95\% \text{ of confidence} \quad (101)$$

i. e.:

$$-140\text{ns} < \text{TIE}(T_m, T_p) < +140\text{ns} \quad \text{with } 95\% \text{ of confidence.} \quad (102)$$

Consequently, a minimal sequence length for the noise level estimation yields a worst confidence interval than with the variance of the residuals (5 times larger here).

- Let us use the whole available sequence (931500s=10.8d) as in figure 8. In this case,  $m=10$ ,  $\nu=8$ ,  $\sigma_y^2(1\text{day}) = 9.7 \times 10^{-26}$ ,  $\hat{k}_{-4} = 4.3 \times 10^{-33}\text{s}^{-1}$  and  $\hat{\sigma}_{TIE}=5.4\text{ns}$ . The corresponding 70% confidence interval is then (see table 7):

$$-1.1\hat{\sigma}_{TIE} < \text{TIE}(T_m, T_p) < +1.1\hat{\sigma}_{TIE} \quad \text{with } 70\% \text{ of confidence} \quad (103)$$

i. e.:

$$-5.9\text{ns} < \text{TIE}(T_m, T_p) < +5.9\text{ns} \quad \text{with } 70\% \text{ of confidence.} \quad (104)$$

For 95% of confidence, we obtain:

$$-2.3\hat{\sigma}_{TIE} < \text{TIE}(T_m, T_p) < +2.3\hat{\sigma}_{TIE} \quad \text{with } 95\% \text{ of confidence} \quad (105)$$

i. e.:

$$-12\text{ns} < \text{TIE}(T_m, T_p) < +12\text{ns} \quad \text{with } 95\% \text{ of confidence.} \quad (106)$$

This demonstrates the necessity to use the maximal available sequence length for estimating the noise levels and then the standard deviation of the TIE.

It may be noticed that it is possible to get even more information about the noise levels, i. e. a narrower confidence interval for the TIE, by using the multivariate method [14] and the total variance concept [15, 16].

## 7 Conclusion

The first application of this work may be the selection of clocks according to their time stability performances. We may fix a limit for the maximum acceptable  $\sigma_\epsilon$  and TIE for a given interpolation sequence and extrapolation time. Let us consider that for an interpolated period  $T_m=24\text{h}$  and for an extrapolated time  $T_p=3.5\text{h}$ , we fix :

$\sigma_e < 2.1$  ns and TIE < 5 ns. The use of equations (57) to (62) allows us to translate the above specifications into specifications on the noise levels  $k_\alpha$  (for instance, for a random walk FM, these specifications become  $k_{-4} < 3.7 \times 10^{-33} \text{s}^{-1}$ ). Furthermore, these specifications may be translated again in term of Allan variance over 1 day (in the case of the random walk FM, it yields  $\sigma_y(24h) < 3 \times 10^{-13}$ ). Thus, we can obtain a very simple criterion by using the Allan variance, ensuring that the specifications for  $\sigma_e$  and TIE will be respected.

Besides the interest of this method for navigation satellite systems, it may be used for defining a new method for very long term stability analysis.

A clock may be continuously measured during a few days (e.g. a time deviation measurement with a sampling period of 1 minute during 10 days). From these data, the noise levels of this clock could be precisely determined [14, 8] and a quadratic fit could be carried out. Thus, if the clock is continuously running in the same conditions, it could be possible to extrapolate the difference of this clock with the parabolic fit after a few months or one year.

This analysis could be helpful to low accuracy purposes of time keeping, for instance for industrialists who periodically send their clock to an accreditation laboratory, or for applications which need a large autonomy.

## APPENDIX 1: Variance of an estimate calculated in the frequency domain

Let us consider an interpolating function  $h(t)$  whose Fourier transform is  $H(f)$ . In the same way as (12), let us denote  $\theta$  the estimate obtained by this interpolated function :

$$\theta = \int_{-\infty}^{+\infty} h(t)x(t)dt. \quad (\text{A1-1})$$

If  $\theta$  is a centered Gaussian random variable, its variance is given by:

$$\langle \theta^2 \rangle = \left\langle \left[ \int_{-\infty}^{+\infty} h(t)x(t)dt \right]^2 \right\rangle. \quad (\text{A1-2})$$

Since  $h(t)$  and  $x(t)$  are real, (A1-2) may be rewritten as:

$$\langle \theta^2 \rangle = \int \int_{-\infty}^{+\infty} \overline{h(t)}h(t') \langle \overline{x(t)}x(t') \rangle dt dt' \quad (\text{A1-3})$$

where the over line denotes a conjugate complex. Let us define  $\tau$  as  $\tau = t' - t$ . The equation (A1-3) may be expressed as a convolution product:

$$\begin{aligned} \langle \theta^2 \rangle &= \int \int_{-\infty}^{+\infty} \overline{h(t)} h(t + \tau) \langle \overline{x(t)} x(t + \tau) \rangle dt d\tau \\ &= \int_{-\infty}^{+\infty} \left( \overline{h(-t)} * h(t) \right)_{(\tau)} \left\langle \left( \overline{x(-t)} * x(t) \right)_{(\tau)} \right\rangle d\tau. \end{aligned} \quad (\text{A1-4})$$

By definition, the convolution product  $\left\langle \left( \overline{x(-t)} * x(t) \right)_{(\tau)} \right\rangle$  is the autocorrelation function  $R_x(t)$  of  $x(t)$ , the Fourier transform of which is the power spectral density  $S_x^{2S}(f)$  (see (26)). On the other hand, the Fourier transform of  $\left( \overline{h(-t)} * h(t) \right)_{(\tau)}$  is  $|H(f)|^2$ . Thus, from the Parseval-Plancherel theorem:

$$\langle \theta^2 \rangle = \int_{-\infty}^{+\infty} |H(f)|^2 S_x^{2S}(f) df = \int_0^{+\infty} |H(f)|^2 S_x(f) df \quad (\text{A1-5})$$

where  $S_x(f)$  is the one-sided power spectral density of  $x(t)$ , see (26).

Whereas this result was obtained with continuous sampled data, it may be applied to discrete sampling by considering the sampling function  $h(t)$  as a sum of Dirac distributions:

$$h(t) = \sum_{i=0}^{N-1} h_i \delta(t - t_i). \quad (\text{A1-6})$$

Therefore,

$$\theta = \int_{-\infty}^{+\infty} h(t) x(t) dt = \sum_{i=0}^{N-1} h(t_i) x(t_i) \quad (\text{A1-7})$$

which is an estimate of the same type as (12).

## APPENDIX 2: The moment condition

Let us consider an interpolating function  $h(t)$  whose Fourier transform is  $H(f)$ . In the same way as (A1-1), this interpolating function is applied to a time deviation sequence  $x(t)$ , the two-sided power spectral density of which is  $S_x^{2S}(f)$ , see (26). This power spectral density is assumed to be modeled by a negative power law, see (29):

$$S_x^{2S}(f) \propto f^\alpha \quad \text{and} \quad \alpha < 0. \quad (\text{A2-1})$$

The variance of the estimate  $\theta$  given by  $h(t)$  applied to  $x(t)$  may be calculated in the frequency domain from (A1-5), as demonstrated in Appendix 1. Therefore, this variance is finite if the following integral converges:

$$\langle \theta^2 \rangle \text{ is finite} \quad \Leftrightarrow \quad \int_{-\infty}^{+\infty} |H(f)|^2 f^\alpha \text{ converges.} \quad (\text{A2-2})$$

This problem with a singularity at zero frequency can be avoided by requiring  $H(f)$  to go to zero for small  $f$ , more rapidly than  $f^{(-\alpha-1)/2}$ . Since the MacLaurin expansion of  $H(f)$  near zero is:

$$H(f) = H(0) + f \left( \frac{dH}{df} \right)_{(f=0)} + \frac{f^2}{2} \left( \frac{d^2H}{df^2} \right)_{(f=0)} + \frac{f^3}{6} \left( \frac{d^3H}{df^3} \right)_{(f=0)} + \dots + \frac{f^q}{q!} \left( \frac{d^qH}{df^q} \right)_{(f=0)} + R_q, \quad (\text{A2-3})$$

the requirement for  $H(f)$  means that the leading  $(-\alpha + 1)/2$  terms of (A2-3) must vanish. As an example, if  $\alpha=-3$ ,  $H(f)$  must go to zero for small  $f$  more rapidly than  $f^1$ , then, the first  $(3 + 1)/2 = 2$  terms of (A2-3) must vanish.

On the other hand,  $H(0)$ ,  $\left( \frac{dH}{df} \right)_{(f=0)}$ ,  $\dots$ ,  $\left( \frac{d^qH}{df^q} \right)_{(f=0)}$  may be calculated in the time domain:

$$\left\{ \begin{array}{l} H(0) = \int_{-\infty}^{+\infty} h(t) dt, \\ \left( \frac{dH}{df} \right)_{(f=0)} = \int_{-\infty}^{+\infty} (-j2\pi t) h(t) dt, \\ \vdots \\ \left( \frac{d^qH}{df^q} \right)_{(f=0)} = \int_{-\infty}^{+\infty} (-j2\pi t)^q h(t) dt. \end{array} \right. \quad (\text{A2-4})$$

Therefore the convergence condition of (A2-2) leads to the following condition [7], called the **moment condition**:

$$\int_{-\infty}^{+\infty} |H(f)|^2 f^\alpha df \text{ converges} \quad \Leftrightarrow \quad \int_{-\infty}^{+\infty} h(t) t^q = 0 \quad \text{for} \quad 0 \leq q \leq \frac{-\alpha - 1}{2}. \quad (\text{A2-5})$$

As in Appendix 1, this condition may be applied to discrete sampling by considering the sampling function  $h(t)$  as a sum of Dirac distributions. The moment condition for discrete sampling is then:

$$\int_{-\infty}^{+\infty} |H(f)|^2 f^\alpha df \text{ converges} \quad \Leftrightarrow \quad \sum_{i=0}^{N-1} h(t_i) t_i^q = 0 \quad \text{for} \quad 0 \leq q \leq \frac{-\alpha - 1}{2}. \quad (\text{A2-6})$$

## Glossary of symbols

$\text{Cov}(x, y)$	Covariance between the random variables $x$ and $y$ .
$[C_v]$	Covariance matrix of the Tchebychev parameters $P_0, P_1$ and $P_2$ .
$C_i$	with $i \in \{0, 1, 2\}$ . The first 3 coefficients of a classical parabola, see (1).
$c_\beta$	Student coefficient for a $\beta\%$ confidence interval.
$e(t)$	Purely random behavior of the time deviation $x(t)$ (by opposition to the deterministic behavior, i. e. the drift).
$\vec{E}$	Vectorial form of $e(t)$ . The components of $\vec{E}$ are the values of $e(t)$ at each measurement time, see (9).
$f$	Fourier frequency variable.
$f_l$	Low cut-off frequency of the spectral density $S_x(f)$ .
$h_\alpha$	Noise level associated with the $f^\alpha$ noise of the power spectral density of frequency deviation $S_y(f)$ .
$h(t)$	Real function of time used as a sampling function.
$H(f)$	Fourier transform of $h(t)$ , i. e. its associated transfer function.
$[I_n]$	The unit matrix $n \times n$ .
$j$	Square root of -1.
$k_\alpha$	Noise level associated with the $f^\alpha$ noise of the power spectral density of time deviation $S_x(f)$ , see (29).
$LG(m, s)$	Laplace-Gauss distribution with a mean value $m$ and a standard deviation $s$ .
$m$	Number of independent sub-sequence of $\tau$ -length in a sequence of time or frequency deviation.
$N$	Number of samples of the interpolated sequence.
$P_i$	with $i \in \{0, 1, 2\}$ . The first 3 Tchebychev parameters.
$\hat{P}_i$	with $i \in \{0, 1, 2\}$ . Estimates of the first 3 Tchebychev parameters.

$\vec{P}$	Vector whose components are the first 3 Tchebychev parameters.
$\vec{\hat{P}}$	Vector whose components are the estimates of the first 3 Tchebychev parameters.
$q$	Integer used as the exponent of the time variable $t$ in the moment condition (see (A2-5) and (A2-6) in Appendix 2).
$R_x(t)$	Autocorrelation function of the time deviation sequence $x(t)$ .
$S_x(f)$	One-sided power spectral density of the time deviation sequence $x(t)$ , see (26).
$S_x^{2S}(f)$	Two-sided power spectral density of the time deviation sequence $x(t)$ . $S_x^{2S}(f)$ is the Fourier transform of the autocorrelation function $R_x(t)$ .
$S_y(f)$	One-sided power spectral density of the frequency deviation sequence $y(t)$ .
TDEV( $\tau$ )	Time deviation of the integration time $\tau$ . Square root of the time variance.
TVAR( $\tau$ )	Time variance of the integration time $\tau$ . See [10].
TIE( $T_m, T_p$ )	Time Interval Error: difference between the extrapolated time deviation and the real time deviation for an interpolated time $T_m$ and an extrapolated time $T_p$ .
$\langle \text{TIE}^2(T_m, T_p) \rangle$	Variance of TIE( $T_m, T_p$ ).
$T_m$	Measurement time: duration of the interpolated sequence, $T_m = N\tau_0$ .
$T_p$	Prediction time: extrapolation time, the origin of which is the beginning of the extrapolated sequence (and the end of the interpolated sequence), see (51).
$t$	Time variable.
$x(t)$	Time deviation sample: the time difference between the real clock under study and an ideal clock at time $t$ , i. e. the gain or the loss of that ideal clock.
$\vec{X}$	Vectorial form of $x(t)$ . The components of $\vec{X}$ are the $N$ time deviation samples, see (7).
$y(t)$	Frequency deviation sample: $y(t) = \frac{dx(t)}{dt}$ .
$\alpha$	Exponent of $f$ for a power law spectral density.
$\beta$	Percentage of confidence for a confidence interval.

$\delta(t)$	Dirac distribution of the argument $t$ .
$\theta$	Estimate obtained by the interpolated function $h(t)$ , see (A1-1).
$\langle \theta^2 \rangle$	Variance of the estimate $\theta$ .
$\nu$	Degrees of freedom of a $\chi^2$ distribution.
$\vec{q}$	Vector whose components are the $N$ residuals of the interpolated sequence, i. e. the differences between the $N$ time deviation samples and the interpolated drift.
$\sigma_e^2$	Variance of the residuals of the interpolated sequence.
$\sigma_{P_i}^2$	Standard deviation of the Tchebychev parameters $P_i$ .
$\sigma_{TIE}$	Real standard deviation of $TIE(T_m, T_p)$ , i. e. square root of $\langle TIE^2(T_m, T_p) \rangle$ .
$\hat{\sigma}_{TIE}$	Estimate of the standard deviation of $TIE(T_m, T_p)$ .
$\sigma_x^2$	Variance of a time deviation sequence composed of white noise (white PM), see (36).
$\sigma_y(\tau)$	Allan deviation for an integration time $\tau$ . Square root of the Allan variance.
$\sigma_y^2(\tau)$	Allan variance for an integration time $\tau$ .
$\tau$	Integration time. Argument of the Allan variance and of TVAR.
$\tau_0$	Sampling period of the time deviation sequence.
$\Phi_i(t)$	with $i \in \{0, 1, 2\}$ . The first 3 Tchebychev polynomials. $i$ is the degree of the polynomial, see (2).
$\vec{\Phi}_i$	Vector whose $N$ components are the values of $\Phi_i(t)$ at each measurement time.
$[\Phi]$	Matrix of the 3 column vectors $\vec{\Phi}_0$ , $\vec{\Phi}_1$ and $\vec{\Phi}_2$ .
$\varphi_i(f)$	Fourier transform of the Tchebychev polynomials $\Phi_i(t)$ .
$\chi_\nu^2$	Chi-square distribution with $\nu$ degrees of freedom.

## References

- [1] J. A. Barnes et al. Characterization of frequency stability. IEEE Transactions on Instrumentation and Measurement, IM-20(2):105–120, May 1971.
- [2] D. W. Allan. Time and frequency (time-domain) characterization, estimation, and prediction of precision clocks and oscillators. IEEE Transactions on Ultrasonics, Ferroelectrics, and Frequency Control, UFFC-34(6):647–654, November 1987.
- [3] L. G. Bernier. Linear prediction of the non-stationary clock error function. In Proceedings of EFTF 88, pages 125–137, Neuchâtel, Switzerland, March 1988.
- [4] L. Di Piro, E. Perone, and P. Tavella. Random walk and first crossing time: applications in metrology. In Proceedings of EFTF 98, pages 388–391, Warsaw, Poland, March 1998.
- [5] A. Lepek. Clock prediction uncertainty. In Proceedings of EFTF 98, pages 205–208, Warsaw, Poland, March 1998.
- [6] J. D. Clarke, J. A. Davis, and J. R. Lavery. UTC and GNSS time scales. In Proceedings of GNSS 2000, Edinburgh, Scotland, UK, May 2000. To be published.
- [7] J. E. Deeter and P. E. Boynton. Techniques for the estimation of red power spectra. I. Context and methodology. The Astrophysical Journal, 261:337–350, October 1982.
- [8] F. Vernotte. Estimation of the power spectral density of frequency deviation samples: Comparison of three methods. In Proceedings of the Joint Meeting of the 13th European Frequency and Time Forum and 1999 IEEE International Frequency Control Symposium, pages 1109–1112, Besançon, Avril 1999.
- [9] F. Vernotte, G. Zalamansky, M. McHugh, and E. Lantz. Cut-off frequencies and noise power law model of spectral density: adaptation of the multi-variance method for irregularly spaced timing data using

the lowest mode estimator approach. IEEE Transactions on Ultrasonics, Ferroelectrics, and Frequency Control, UFFC-43(3):403–409, May 1996.

- [10] D.W. Allan, M.A. Weiss, and J.L. Jespersen. A frequency-domain view of time-domain characterization of clocks and time and frequency distribution systems. In Proceedings of the 45th IEEE Frequency Control Symposium, pages 667–678, May 1991.
- [11] G. Saporta. Probabilités, analyse des données et statistique. Editions Technip, Paris, 1990. ISBN 2-7108-0565-0.
- [12] P. Lesage and C. Audoin. Characterization of frequency stability: uncertainty due to the finite number of measurements. IEEE Transactions on Instrumentation and Measurement, IM-22(2):157–161, June 1973. See also comments in IM-24 p. 86 and correction in IM-25 p. 270.
- [13] D. A. Howe, D. W. Allan, and J. A. Barnes. Properties of signal sources and measurement methods. In Proceedings of the 35th IEEE Frequency Control Symposium, pages A25–A35, Philadelphia, PA, USA, May 1981.
- [14] F. Vernotte, E. Lantz, J. Gros Lambert, and J.J. Gagnepain. Oscillator noise analysis: multivariate measurement. IEEE Transactions on Instrumentation and Measurement, 42(2):342–350, Avril 1993.
- [15] C. A. Greenhall, D. A. Howe, and D. B. Percival. Total variance, an estimator of long-term frequency stability. IEEE Transactions on Ultrasonics, Ferroelectrics, and Frequency Control, 46(5):1183–1191, September 1999.
- [16] D.A. Howe. The total deviation approach to long-term characterization of frequency stability. IEEE Transactions on Ultrasonics, Ferroelectrics, and Frequency Control, 47(5):1102–1110, September 2000.

## List of Tables

1	Convergence of the $P_i$ parameters versus the type of noise. A star $\star$ denotes the convergence. .	37
2	Correlations of the time deviation data $x(t)$ versus the noise levels $k_\alpha$ . $C$ is the Euler constant: $C \approx 0,5772$ . Assuming a sampling satisfying the Shannon rule, the high cut-off frequency is $f_h = \frac{1}{2\tau_0}$ . $f_l$ is the low cut-off frequency. . . . .	38
3	Summary of the theoretical results. . . . .	39
4	Comparison between the Time Variance TVAR( $\tau$ ) and the variance of the residuals $\sigma_e^2$ for different types of noise and for quadratic and linear interpolation. . . . .	40
5	Comparison between measured and estimated values of $\sigma_e$ and $\sigma_{TIE}$ for several clocks with a quadratic interpolation. . . . .	41
6	Comparison between measured and estimated values of $\sigma_e$ and $\sigma_{TIE}$ for two Cesium clocks with a linear interpolation. . . . .	42
7	Degrees of freedom of $\hat{\sigma}_e^2$ and $\hat{\sigma}_{TIE}$ , and confidence coefficients $c_\beta$ for 70% and 95% versus the types of noise [11]. . . . .	43

$S_x(f)$	$k_0 f^0$	$k_{-1} f^{-1}$	$k_{-2} f^{-2}$	$k_{-3} f^{-3}$	$k_{-4} f^{-4}$
$P_0$	*				
$P_1$	*	*	*		
$P_2$	*	*	*	*	*

Table 1: Convergence of the  $P_i$  parameters versus the type of noise. A star  $*$  denotes the convergence.

$S_x(f)$	$R_x(t_j - t_i)$ (with $i \neq j$ )	$R_x(0)$
$k_{-4} \cdot f^{-4}$	$k_{-4} \left[ \frac{1}{3f_l^3} - \frac{2\pi^2}{f_l} (t_j - t_i)^2 + \frac{2\pi^4}{3}  t_j - t_i ^3 \right]$	$\frac{k_{-4}}{3f_l^3}$
$k_{-3} \cdot f^{-3}$	$k_{-3} \left[ \frac{1}{2f_l^2} + \pi^2 (t_j - t_i)^2 \{-3 + 2C + 2 \ln(2\pi f_l  t_j - t_i )\} \right]$	$\frac{k_{-3}}{2f_l^2}$
$k_{-2} \cdot f^{-2}$	$k_{-2} \left[ \frac{1}{f_l} - \pi^2  t_j - t_i  + 2\pi^2 f_l (t_j - t_i)^2 \right]$	$\frac{k_{-2}}{f_l}$
$k_{-1} \cdot f^{-1}$	$k_{-1} \left[ -C - \ln(2\pi f_l  t_j - t_i ) + \pi^2 f_l^2 (t_j - t_i)^2 \right]$	$k_{-1} \ln \left( \frac{f_h}{f_l} \right)$
$k_0$	0	$k_0 f_h$

Table 2: Correlations of the time deviation data  $x(t)$  versus the noise levels  $k_\alpha$ .  $C$  is the Euler constant:  $C \approx 0,5772$ . Assuming a sampling satisfying the Shannon rule, the high cut-off frequency is  $f_h = \frac{1}{2T_0}$ .  $f_l$  is the low cut-off frequency.

$S_x(f)$	$k_{-2}f^{-2}$	$k_{-3}f^{-3}$	$k_{-4}f^{-4}$
$R_x(t)$	See Table 2 page 38		
$\sigma_{P_1}^2$	(53) page 13	-	-
$\sigma_{P_2}^2$	(54) page 13	(55) page 13	(56) page 13
Quadratic interpolation			
$\sigma_e^2$	(57) page 14	(58) page 14	(59) page 14
$\langle \text{TIE}^2(T_m, T_p) \rangle$ (from $k_\alpha$ )	(60) page 14	(61) page 14	(62) page 15
$\langle \text{TIE}^2(T_m, T_p) \rangle$ (from $\sigma_e^2$ )	(63) page 15	(64) page 15	(65) page 15
$\lim_{T_p \rightarrow \infty} \langle \text{TIE}^2(T_m, T_p) \rangle$	(66) page 16	(67) page 16	(68) page 16
Linear interpolation			
$\sigma_e^2$	(71) page 17	(72) page 17	(73) page 17
$\langle \text{TIE}^2(T_m, T_p) \rangle$ (from $k_\alpha$ )	(74) page 17	(75) page 17	(76) page 18
$\langle \text{TIE}^2(T_m, T_p) \rangle$ (from $\sigma_e^2$ )	(77) page 18	(78) page 18	(79) page 18
$\lim_{T_p \rightarrow \infty} \langle \text{TIE}^2(T_m, T_p) \rangle$	(80) page 18	(81) page 18	(82) page 19

Table 3: Summary of the theoretical results.

$S_x(f)$	$k_{-2}f^{-2}$	$k_{-3}f^{-3}$	$k_{-4}f^{-4}$
$\text{TVAR}(\tau)$	$\frac{\pi^2 k_{-2} \tau}{3}$	$\frac{\pi^2 [27 \ln(3) - 32 \ln(2)] k_{-3} \tau^2}{6}$	$\frac{11 \pi^4 k_{-4} \tau^3}{15}$
Quadratic interpolation			
$\sigma_e^2$	$\frac{3 \pi^2 k_{-2} \tau}{35}$	$\frac{\pi^2 k_{-3} \tau^2}{24}$	$\frac{\pi^4 k_{-4} \tau^3}{315}$
$\frac{\sigma_e^2}{\text{TVAR}(\tau)}$	$\frac{9}{35}$	$\frac{1}{4 [27 \ln(3) - 32 \ln(2)]}$	$\frac{1}{231}$
$\frac{\text{TDEV}(\tau)}{\sigma_e^2}$	0.51	0.18	0.066
Linear interpolation			
$\sigma_e^2$	$\frac{2 \pi^2 k_{-2} \tau}{15}$	$\frac{\pi^2 k_{-3} \tau^2}{9}$	$\frac{6 \pi^4 k_{-4} \tau^3}{315}$
$\frac{\sigma_e^2}{\text{TVAR}(\tau)}$	$\frac{2}{5}$	$\frac{2}{3 [27 \ln(3) - 32 \ln(2)]}$	$\frac{2}{77}$
$\frac{\text{TDEV}(\tau)}{\sigma_e^2}$	0.63	0.30	0.16

Table 4: Comparison between the Time Variance  $\text{TVAR}(\tau)$  and the variance of the residuals  $\sigma_e^2$  for different types of noise and for quadratic and linear interpolation.

Clock	$\sigma_y(24\text{h})$	$h_{-2}$ ( $\text{s}^{-1}$ )	$h_{-1}$	$h_0$ (s)	$\sigma_e$ exp. (ns)	$\sigma_e$ theo. (ns)	$\sigma_{TIE}$ exp. (ns)	$\sigma_{TIE}$ theo. (from $h_\alpha$ ) (ns)	$\sigma_{TIE}$ theo. (from $\sigma_e$ ) (ns)
Quartz 1	$1.8 \times 10^{-13}$	0	$2.2 \times 10^{-26}$	$7.5 \times 10^{-23}$	1.4	1.4	7.1	6.2	6.6
Quartz 2	$2.9 \times 10^{-12}$	$1.4 \times 10^{-29}$	$1.6 \times 10^{-25}$	0	9.6	9.2	56.5	52.0	56.0
Quartz 3	$3.0 \times 10^{-12}$	$1.4 \times 10^{-29}$	$6.4 \times 10^{-25}$	0	10.2	11.0	55.7	59.0	59.5
Rb 1	$2.7 \times 10^{-13}$	$1.2 \times 10^{-31}$	0	$5.3 \times 10^{-22}$	1.2	1.3	6.2	5.7	7.1
Cs 1	$9.2 \times 10^{-14}$	0	0	$1.5 \times 10^{-21}$	1.7	1.6	5.5	5.5	5.6
Cs 2	$3.0 \times 10^{-14}$	0	$2.1 \times 10^{-28}$	$1.1 \times 10^{-22}$	0.6	0.5	1.9	1.6	3.0

Table 5: Comparison between measured and estimated values of  $\sigma_e$  and  $\sigma_{TIE}$  for several clocks with a quadratic interpolation.

Clock	$\sigma_y(24\text{h})$	$h_{-1}$	$h_0$ (s)	$\sigma_e$ exp. (ns)	$\sigma_e$ theo. (ns)	$\sigma_{TIE}$ exp. (ns)	$\sigma_{TIE}$ theo. (from $h_\alpha$ ) (ns)	$\sigma_{TIE}$ theo. (from $\sigma_e$ ) (ns)
Cs 1	$9.2 \times 10^{-14}$	0	$1.5 \times 10^{-21}$	2.0	2.1	4.1	4.6	4.5
Cs 2	$3.0 \times 10^{-14}$	$2.1 \times 10^{-28}$	$1.1 \times 10^{-22}$	0.8	0.6	1.5	1.4	1.8

Table 6: Comparison between measured and estimated values of  $\sigma_e$  and  $\sigma_{TIE}$  for two Cesium clocks with a linear interpolation.

$S_x(f)$	$\nu$	$c_{70\%}$	$c_{95\%}$
$k_{-2}f^{-2}$	8	1.1	2.3
$k_{-3}f^{-3}$	3	1.2	3.2
$k_{-4}f^{-4}$	2	1.4	4.3

Table 7: Degrees of freedom of  $\hat{\sigma}_e^2$  and  $\hat{\sigma}_{TIE}$ , and confidence coefficients  $c_\beta$  for 70% and 95% versus the types of noise [11].

**List of Figures**

1 Quadratic fit over a time deviation sequence of white FM (above). The fit is performed over the first quarter of the sequence. The residuals of this fit (below) corresponds to our definition of TIE. 45

2 Dispersion of the TIE for 20 realizations of the same white FM process (above). The histogram of 10000 realizations of the TIE estimates (here for  $t = 40000$ s) exhibits a Gaussian behavior (below). . . . . 46

3 The first 3 Tchebychev polynomials calculated for  $N = 100$  data. . . . . 47

4 Comparison of the estimation of the standard deviation of the TIE calculated from the equation (60), (61), (62), (74), (75), (76) (solid lines) and estimated over 10000 realizations of simulated noise for a quadratic interpolation ( $\circ$ ,  $\times$ , and  $\square$ ) and for a linear interpolation ( $*$ ,  $\diamond$  and  $+$ ). In order to use the same scale, the noise levels were defined in such a way that the variance of the residuals is equal to one ( $k_{-2} = 1.4 \times 10^{-4}$ s,  $k_{-3} = 3.3 \times 10^{-8}$  and  $k_{-4} = 5.0 \times 10^{-12}$ s $^{-1}$  for the quadratic interpolation,  $k_{-2} = 3.5 \times 10^{-3}$ s,  $k_{-3} = 4.8 \times 10^{-7}$  and  $k_{-4} = 3.3 \times 10^{-11}$ s $^{-1}$  for the linear interpolation). The error bars corresponding to the estimates of the simulated noises are too small to be plotted on this graph. The lower plot shows the differences between the theoretical curves and the simulation points: the larger error is equal to 5% but most of them are below 1%. . . . . 48

5 Evolution of the TIE after the fitted sequence for an ultra-stable quartz oscillator. The fit was performed over 1 day with a sampling period of 10s. The estimation of the TIE (dashed line) was performed from equation (60) and (62) by using the noise level estimates:  $k_{-2} = 2.5 \times 10^{-24}$ s ( $h_0 = 9.9 \times 10^{-23}$ s) and  $k_{-4} = 4.0 \times 10^{-33}$ s $^{-1}$  ( $h_{-2} = 1.6 \times 10^{-31}$ s $^{-1}$ ). These levels were estimated with the Allan variance over a 5 days sequence. The lower graph is an enlargement of the first 4 hours of the upper plot. . . . . 49

6 Estimation of the TIE for the same oscillator as fig. 5. The fit was performed over a 1 day sliding window. The TIE was measured 3.5 hours after the fitted sequence (solid line). The TIE bounds (dashed lines) were estimated from the noise levels (above) or from the variance of the residuals (below). . . . . 50

7 Cumulative distribution function of the real TIE expressed in  $\hat{\sigma}_{TIE}$  units (e. g. 2 means 2  $\hat{\sigma}_{TIE}$ ). The estimate  $\hat{\sigma}_{TIE}$  was obtained from the variance of the residuals  $\hat{\sigma}_e^2$ . The upper graph shows the probability curves for the 3 low frequency noises. The lower graph compares the probability of the TIE for a  $f^{-4}$  PM with the probability of  $\chi^2$  laws with 1 degree of freedom and with 2 degrees of freedom. As an example, whereas the probability of a random variable to be smaller than  $-1\sigma$  is 16% for a Laplace Gauss law, 21% for a  $\chi_2^2$  law and 25% for a  $\chi_1^2$  law, the probability of the real TIE to be smaller than  $-1\hat{\sigma}_{TIE}$  (to be under the lower bounds of figures 5 and 6) is 24%. . . . . 51

8 Allan variance plot of the clock Rb 1 (see table 5). The fit and the spectral analysis were performed by using the multivariate method [14], including the Allan variance, the Picinbono variance and the modified Allan variance. The sampling period was 1 s and the length of the sequence 10.8 days (931500 data). . . . . 52

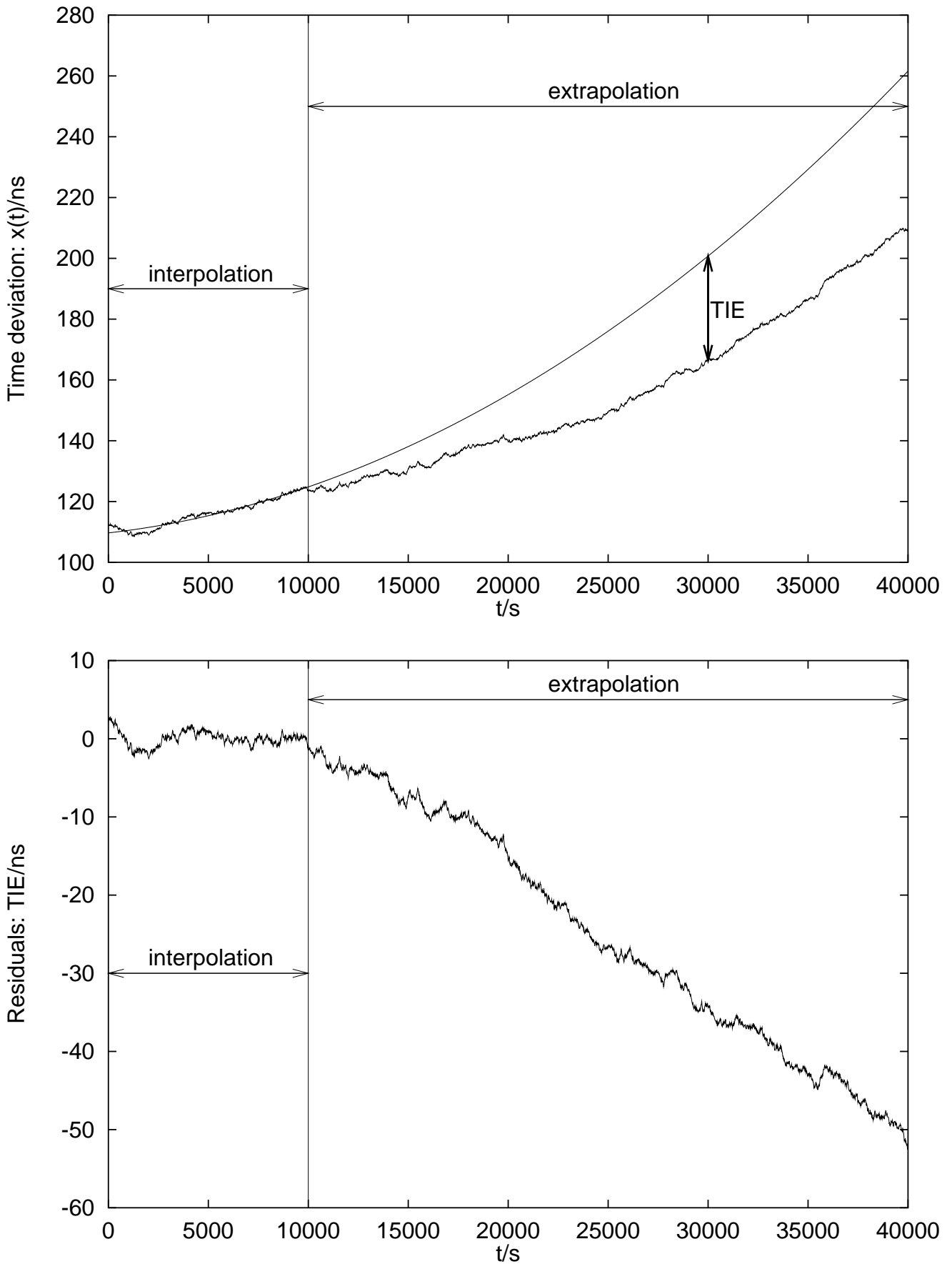


Figure 1: Quadratic fit over a time deviation sequence of white FM (above). The fit is performed over the first quarter of the sequence. The residuals of this fit (below) corresponds to our definition of TIE.

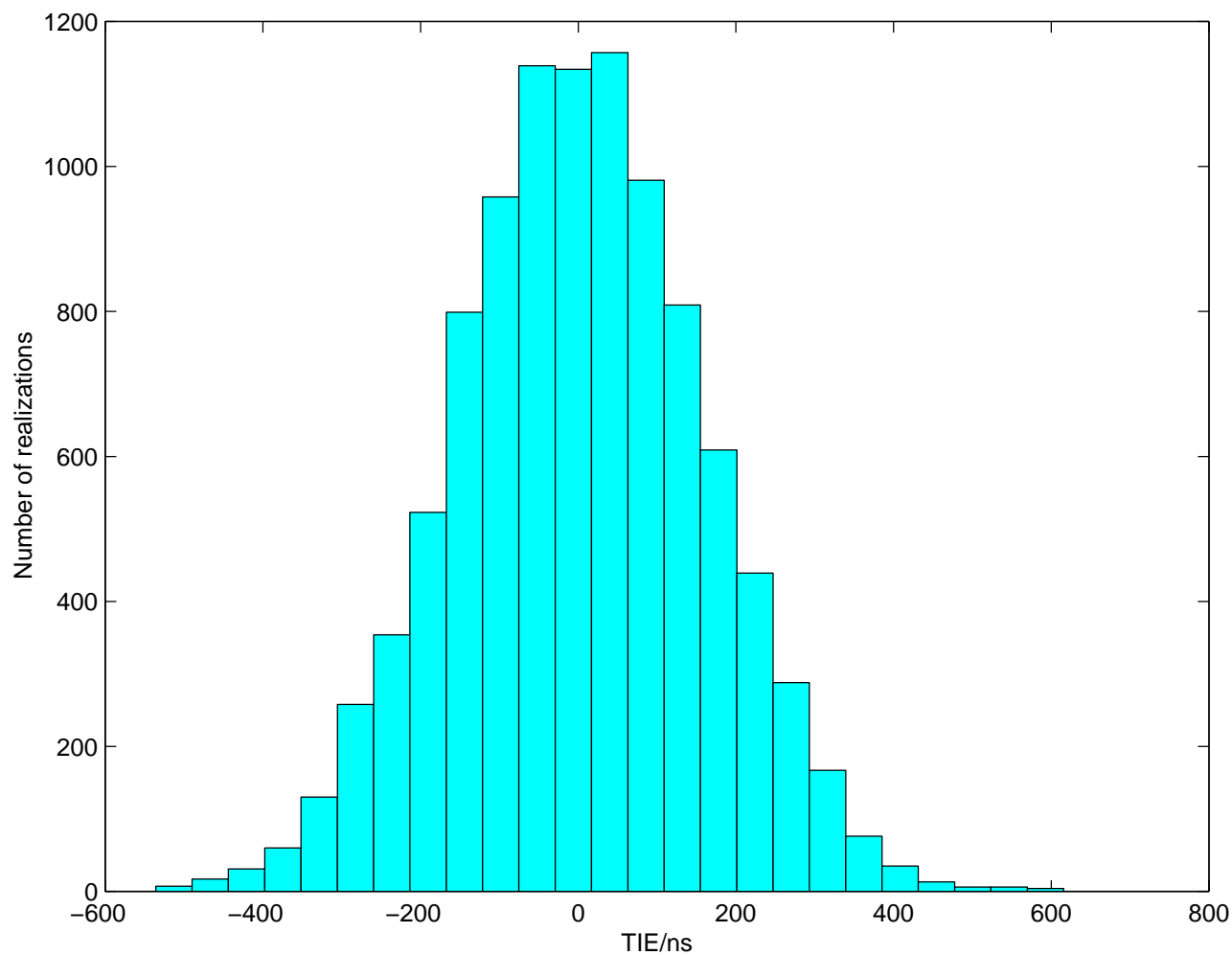
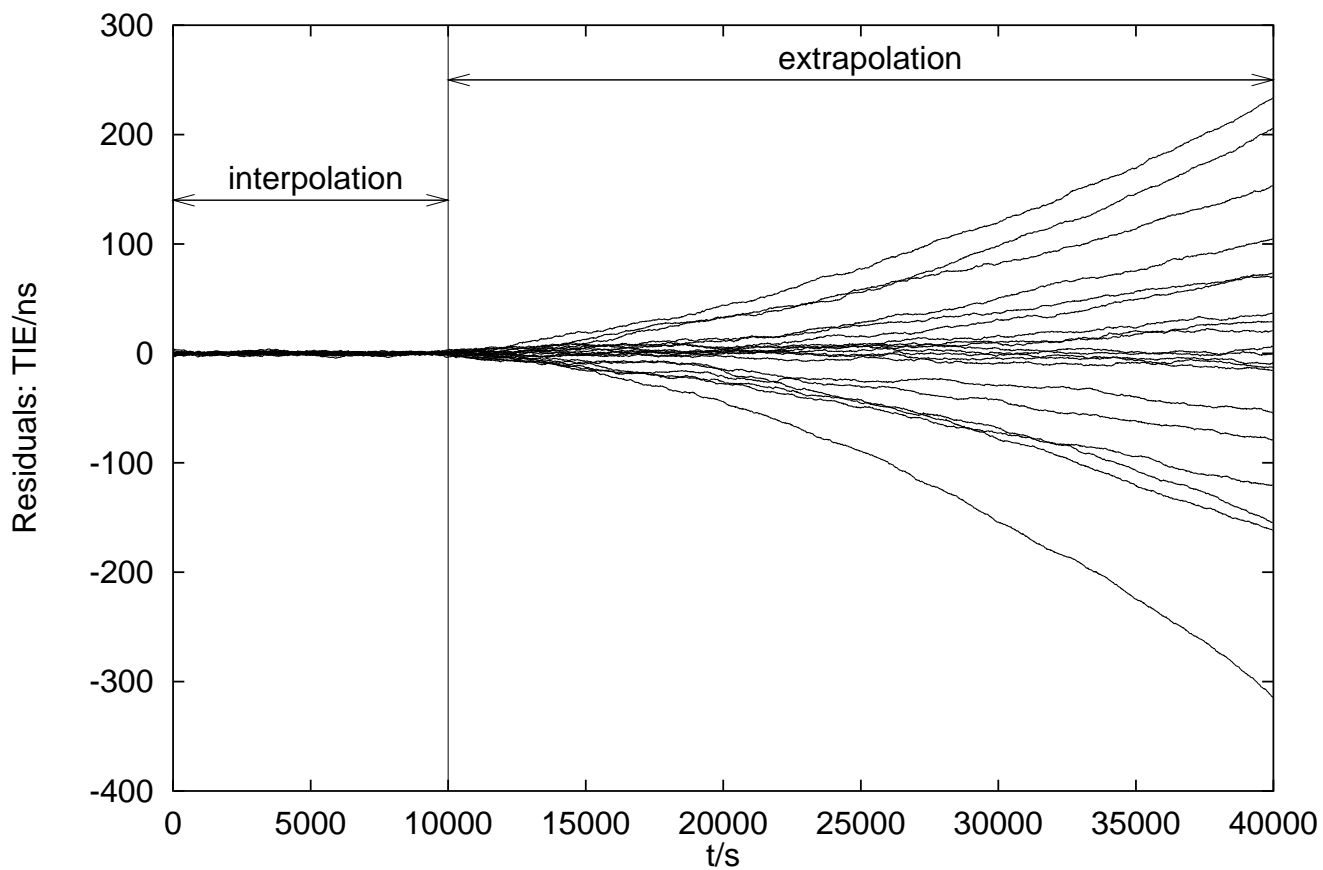


Figure 2: Dispersion of the TIE for 20 realizations of the same white FM process (above). The histogram of

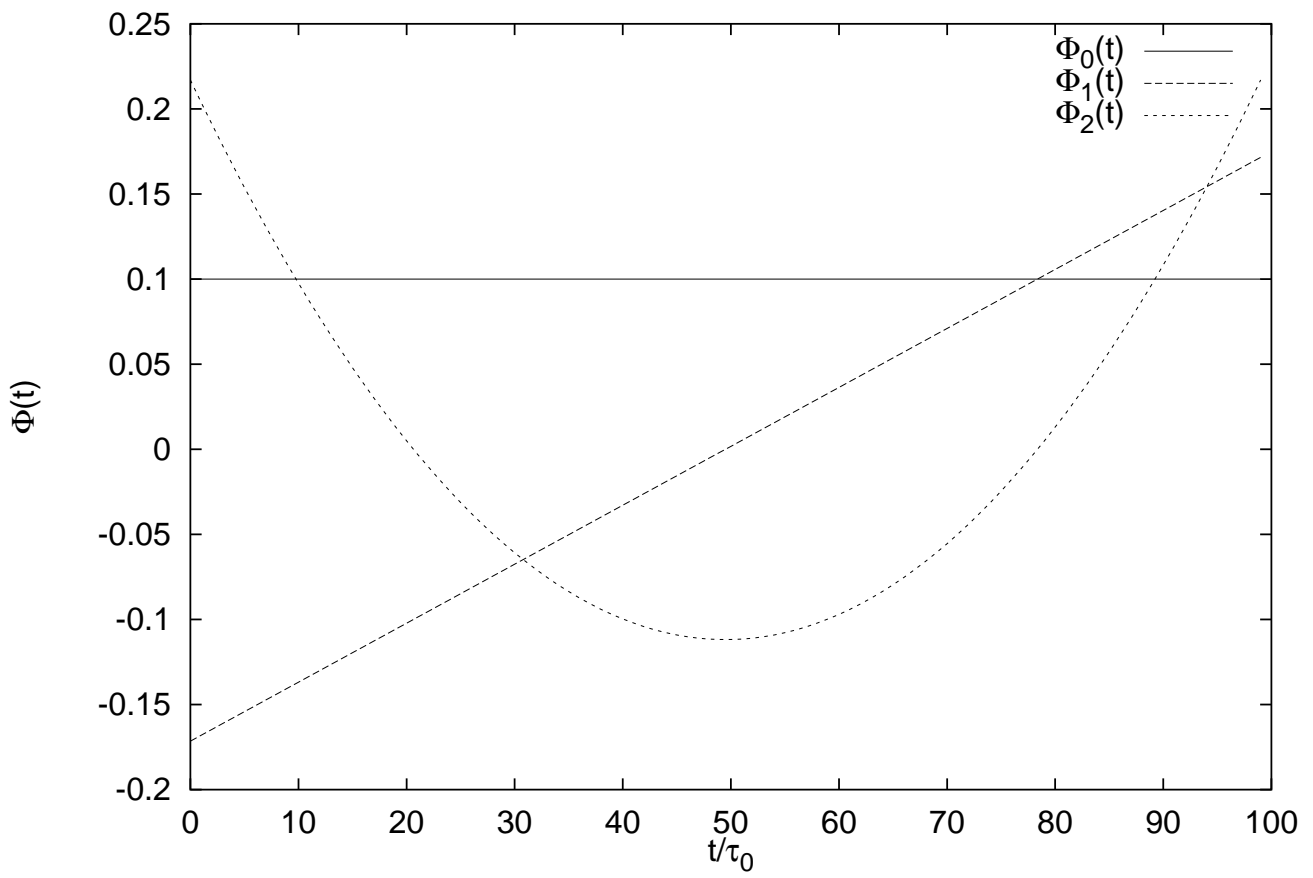


Figure 3: The first 3 Tchebychev polynomials calculated for  $N = 100$  data.

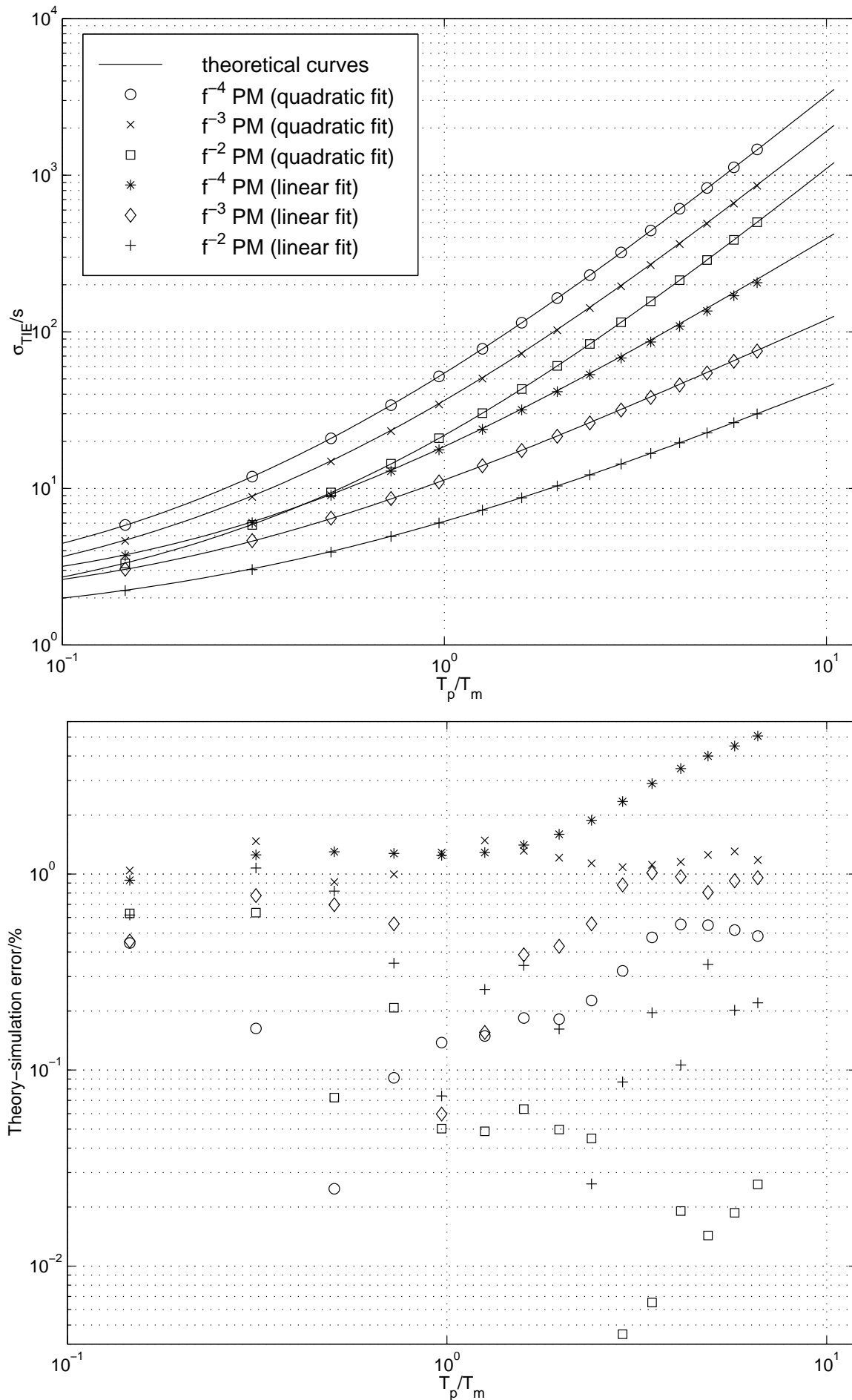


Figure 4: Comparison of the estimation of the standard deviation of the TIE calculated from the equation (60), (61), (62), (74), (75), (76) (solid lines) and estimated from 10000 realizations of simulated data for a quadratic

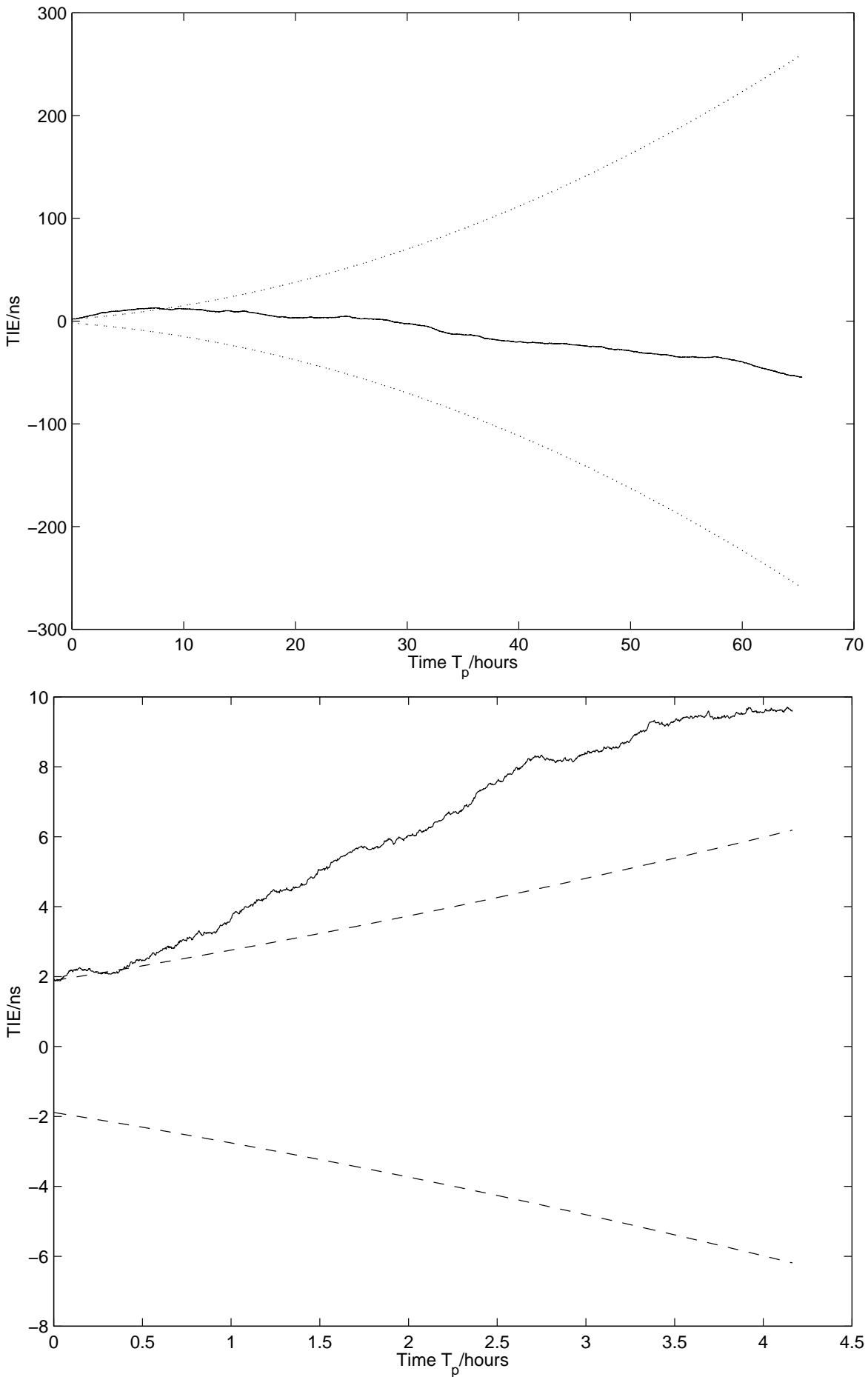


Figure 5: Evolution of the TIE after the fitted sequence for an ultra-stable quartz oscillator. The fit was performed over 1 day with a sampling period of 10s. The estimation of the TIE (dashed line) was performed from equation (60) and (62) by using the noise level estimates:  $h_{11} = 2.5 \times 10^{-24} \text{s}^{-2}$ ,  $h_{22} = 0.0 \times 10^{-23} \text{s}^{-2}$  and

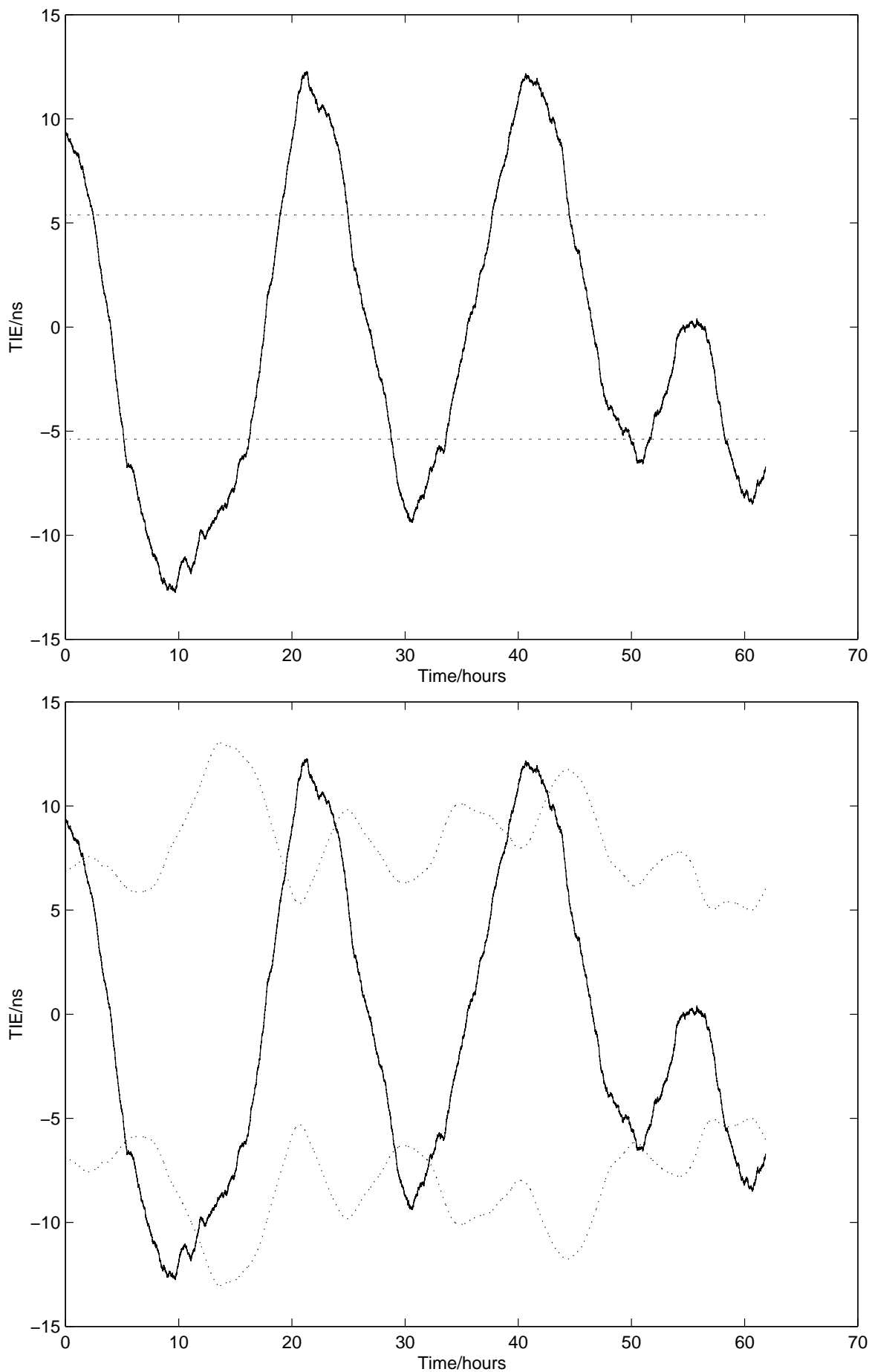


Figure 6: Estimation of the TIE for the same oscillator as fig. 5. The fit was performed over a 1 day sliding window. The TIE was measured 3.5 hours after the fitted sequence (solid line). The TIE bounds (dashed lines) were estimated from the noise levels (above) or from the variance of the residuals (below).

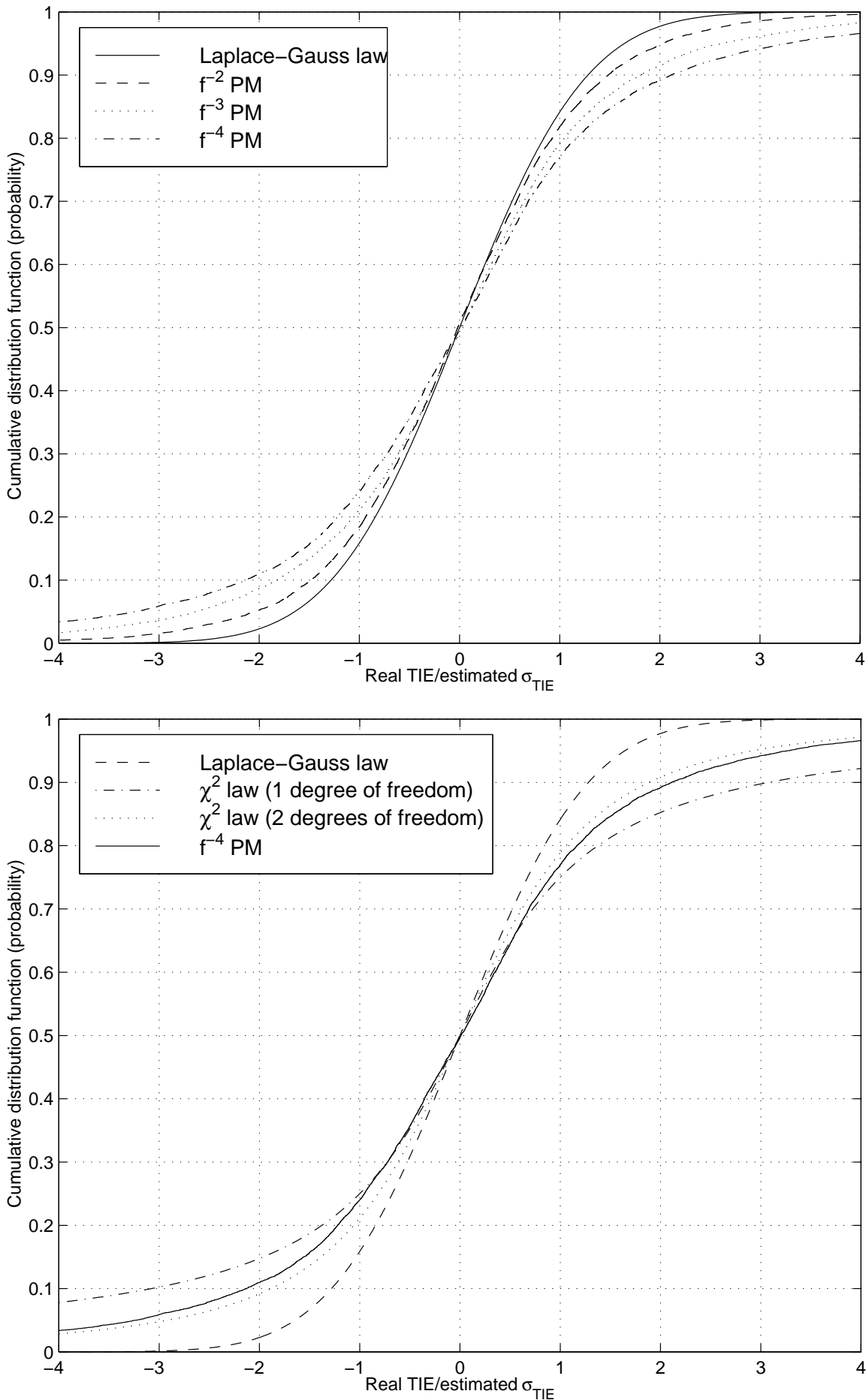


Figure 7: Cumulative distribution function of the real TIE expressed in  $\hat{\sigma}_{TIE}$  units (e. g. 2 means  $2 \hat{\sigma}_{TIE}$ ). The estimate  $\hat{\sigma}_{TIE}$  was obtained from the variance of the residuals  $\hat{\sigma}_e^2$ . The upper graph shows the probability

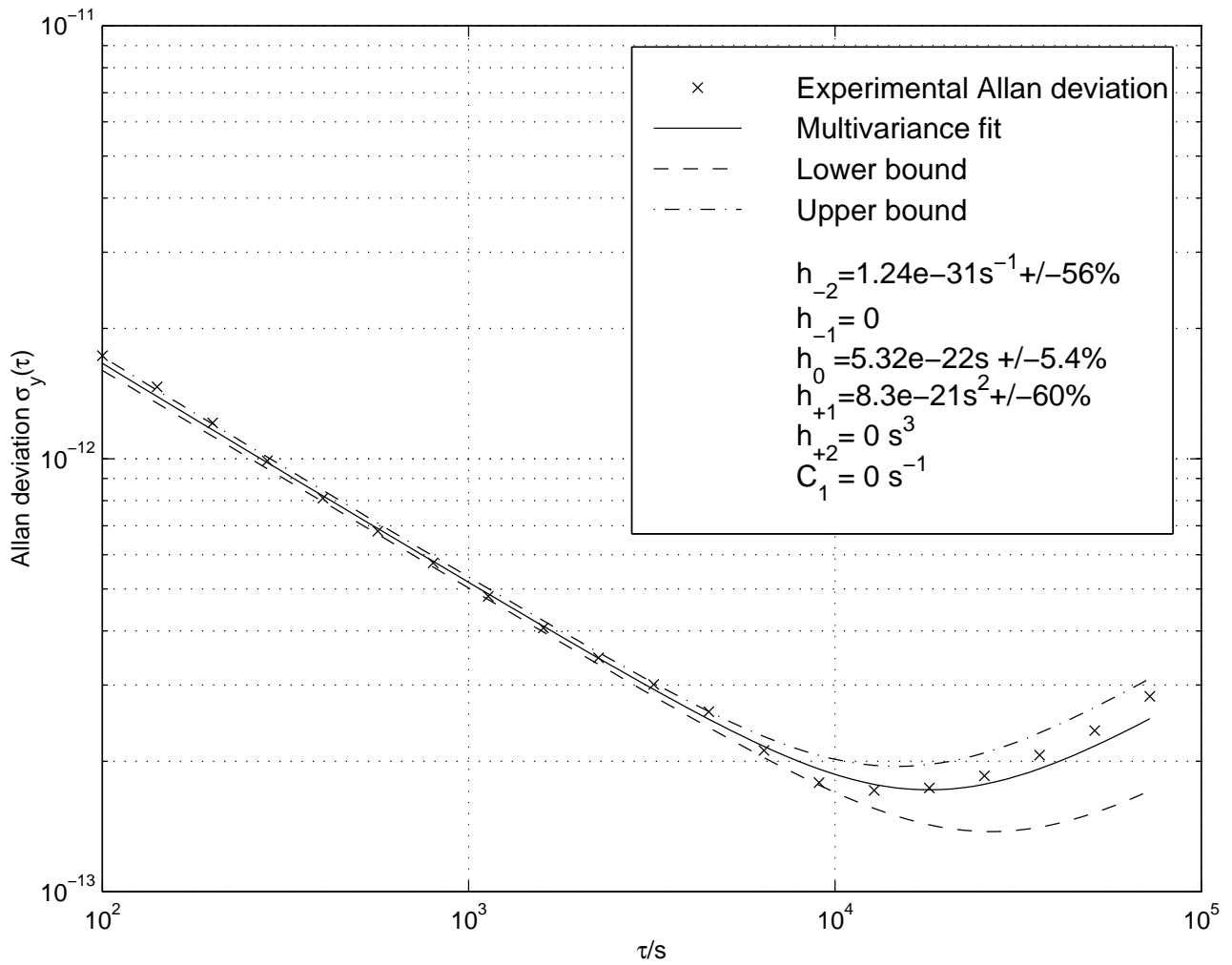


Figure 8: Allan variance plot of the clock Rb 1 (see table 5). The fit and the spectral analysis were performed by using the multivariate method [14], including the Allan variance, the Picinbono variance and the modified Allan variance. The sampling period was 1 s and the length of the sequence 10.8 days (931500 data).